DEPARTMENT OF CHEMISTRY, UNIVERSITY OF JYVÄSKYLÄ
RESEARCH REPORT No. 173

STRUCTURAL STUDIES OF DIELECTRIC POLYMER NANOCOMPOSITES

BY

SUVI VIRTANEN

Academic Dissertation for the Degree of
Doctor of Philosophy

To be presented, by permission of the Faculty of Mathematics and Science of the University of Jyväskylä, for public examination in Auditorium KEM4, on December 13th, 2013 at 12 noon.

UNIVERSITY OF JYVÄSKYLÄ

ISBN 978-951-39-5508-3 (nid.)
ISBN 978-951-39-5584-7 (PDF)
URN:ISBN:978-951-39-5584-7
ISSN 0357-346X

ABSTRACT

Virtanen, Suvi
Structural studies of dielectric polymer nanocomposites
Jyväskylä: University of Jyväskylä, 2013, 61 p.
Department of Chemistry, University of Jyväskylä Research Report
ISSN 0357-346X; 173
ISBN 978-951-39-5508-3 (nid.), 978-951-39-5584-7 (PDF)
Diss.

A constant need for the development of new and superior materials is always present; for example, a better electrical insulator would enable more efficient use of electrical power. Polymeric nanocomposites, i.e. nanodielectrics, are thought to have unique electrical properties. The basic chemical constitution of a material alone fails to provide an understanding of how desired properties of a material originate or predict the long term behavior of a material. We need to define the structure behind the functionality of a material. To do that, the structure of the material must be studied on several scales. This research was part of the Finnish Funding Agency for Technology and Innovation (TEKES) consortium projects NANOCOM and NANOPOWER. The general objective of these projects was to create truly new theoretical, experimental and practical knowledge of novel polymer nanocomposites to be further developed and finally used both in electrical and electronics insulation technology, as well as in other fields of technology.

Raman imaging was found to be a good tool for studying the structure of the materials: it provides information on the chemical species as well as dispersion of the filler. Alongside traditional confocal Raman imaging, which gives detailed information even at the submicron scale, coarse Raman imaging was used allowing the screening of a large area from a sample which is important for quality control of the composites to be used in industrial scale.

A new synthetic approach was used to afford well-dispersed silica particles with electroactive core functionalization in epoxy in order to study the effect of the charge layer at the interface of nanoparticle and polymer matrix. If the achieved distribution of particles was dense enough, the dielectric breakdown strength (DBS) increased considerably. The demonstrated increase in DBS and permittivity of the material leads to an increase of up to 125% in theoretical capacitive energy storage capability, and this is promising for future applications. These changes in properties are achieved with only 2 wt-% filler loading. Dielectric losses in the frequency range critical to the planned application stayed at the level of unfilled epoxy. This work is the first step towards new type functionalization of filler that offers good dispersion of nanoparticles without using harsh mixing conditions. These preliminary results indicate that the charge layer in the nanoparticle core, alongside a sufficiently dense enough distribution of particles at nanoscale, could be one way to improve dielectric properties of polymer materials.

Keywords: nanodielectrics, polymer nanocomposite, dispersion, transmission electron microscopy, Raman microscopy

Author's address Suvi Virtanen
Nanoscience Center
Department of Chemistry
University of Jyväskylä
Finland

Supervisor Prof. Mika Pettersson
Nanoscience Center
Department of Chemistry
University of Jyväskylä
Finland

Reviewers Dos. Anna-Stiina Jääskeläinen
VTT Technical Research Centre of Finland
Finland

Prof. Tuula Pakkanen
Department of Chemistry
University of Eastern Finland
Finland

Opponent Prof. Alun Vaughan
Electrical and Computational Sciences
Faculty of Physical and Applied Sciences
University of Southampton
United Kingdom

PREFACE

The work presented in this thesis has been carried out at the Department of Chemistry, Nanoscience Center at the University of Jyväskylä during the years 2008-2013. For the last manuscript the research is done during 10 months ASLA-Fulbright Pre-Doctoral Research Fellows visit at Rensselaer Polytechnic Institute (RPI), Troy, NY 2012-2013.

The work has been financially supported by the Finnish Funding Agency for Technology and Innovation (TEKES), the Magnus Ehrnrooth Foundation, Fulbright Center Finland and University of Jyväskylä, which are all gratefully acknowledged.

First I would like to thank my supervisor Prof. Mika Pettersson for giving me opportunity to step in to this challenge, and also for being such a great role model. There were so many people that provided help and the work that they have done, has kept this research going forward. No amount of gratitude could ever be too much for XPD study and support I have got from Adj. Prof. Manu Lahtinen. I wish to express my gratitude to Dr. Viivi Nuottajärvi for tomography analysis; you had such a deep interest to do it. MSc. Tuomas Turpeinen was an indispensable help in particle analysis; you were there always to help me in the hour of need. I could not have done this without your help. TEM lab technicians: Paavo Niutanen and Petri Papponen are greatly appreciated. MSc. Susanna Ahonen stepped in to the project during time of my maternity leave and did such a great job at it. MSc. Jaakko Koivisto is remembered for all the help he has given me over the years.

My collaborators were the key to accomplish any results: most the dielectric analysis of the studied materials and theoretical calculations relying on the experimental results are conducted in Tampere University of Technology (TUT). The dielectric materials were manufactured at the Technical Research Centre of Finland (VTT), so, I was fortuned to have a strong interdisciplinary collaboration network providing support. Especially I want to thank Dr. Markus Takala for the introduction to the field of electrical testing and also being so good company. MSc. Hannes Ranta is also sincerely acknowledged for the dielectrical testing. I am grateful for MSc. Tommi Kortelainen to have the patience and wisdom to help me understand the great mysteries on computational chemistry; it was truly a pleasure to work with you. I would like especially want to thank late Assoc. Prof. Kari Kannus for encouraging me to try to go on exchange visit to RPI and of course Prof. emer. J. Keith Nelson and Prof. Linda S. Schadler for giving me opportunity to work there; you were great. I had opportunity to try so many new things! It was a life changing experience for me and my family, and we will never forget it. I will cherish the hours in the basement of Materials Research Center (MRC) with Prof. emer. Robert MacCrone and Prof. emer. J. Keith Nelson and the EPR setup. I got also a chance to work alongside with Timothy Krentz: thank you for all the times you helped me to start all over again after everything seemed gone wrong. Thousands of thanks go to the whole Bullpen at MRC for camping gear and all the support I got during my

visit. I want to acknowledge Dr. Robert Smith for guiding me in pulsed electro acoustic analysis, Michael Goodman for all the time you spent teaching us voltage endurance testing, Michael Topka for the tests we did with "click- reaction". I sincerely want to thank Michael Bell from University of South Carolina for providing me "long and short brushes". I will also remember the valuable discussions over the phone with Assoc. Prof. Henrik Hillborg.

I appreciate my colleagues at Physical Chemistry and Nanoscience Center for the nice atmosphere; especially university teachers and Dr. Saara Kaski and Dr. Tiina Kiviniemi, MSc. Päivi Ruokola, Dr. Riikka Reitzer have been a real support to me during these years.

I am truly grateful for my friends and family. The support from my parents; Kari and Tuija has been solid. I want to thank my children Senja and Angus for being born and my husband Ian for love and support.

Jyväskylä, November 2013
Suvi Virtanen

LIST OF ORIGINAL PUBLICATIONS

The main results in this thesis have been reported in the following publications and they are herein referred by their Roman numerals (I-IV).

I M. Takala, H. Ranta, P. Nevalainen, P. Pakonen, J. Pelto, M. Karttunen, S. Virtanen, V. Koivu, M. Pettersson, B. Sönerud, K. Kannus, Dielectric properties and partial discharge endurance of polypropylene-silica nanocomposite, *IEEE Trans. Dielectr. Electr. Insul.* **2010,** 14, 4, 1259-1267

II S. Virtanen, T. Kortelainen, S. Ahonen, V. Koivu, M. Lahtinen, E. Arola, S. Kortet, M. Karttunen, K. Kannus, M. Pettersson, Characterization of octamethylsilsesquioxane $(CH_3)_8Si_8O_{12}$ fillers in polypropene matrix. *22nd Nordic Insulation Symposium*, NORD-IS11, **2011**, Tampere, Finland.

III S. Virtanen, H. Ranta, S. Ahonen, M. Karttunen, J. Pelto, K. Kannus and M. Pettersson, The structure and dielectric properties of nano-$CaCO_3$/polypropylene composites. *J.Appl. Pol.Sci.* **2014**, 131, 1, 39504

IV S. Virtanen, T. Krentz, L. S. Schadler, J. K. Nelson, M. Bell, B. Benicewicz, H. Hilborg and S. Zhau, Dielectric Breakdown Strength of Epoxy Bimodal-Polymer-Brush-Grafted Core Functionalized Silica Nanocomposites submitted to *IEEE Trans. Dielectr. Electr. Insul.*

Author's contribution

In Publication I the Author has either done or coordinated the structural analysis and written the corresponding part of the paper. In publication II the Author has done or coordinated the experimental part and has written the paper. In publication III the Author has done all the structural characterization and written the paper. In publication IV the Author has done the nanoparticle surface modification syntheses, structural characterization and participated in composite processing and electrical testing. The Author has also written the first draft of the manuscript.

ABBREVIATIONS

AC	alternating current
DBS	dielectric breakdown strength
DC	direct current
DMF	dimethylformamide
CXμT	computerized x-ray micro-tomography
NNI	nearest neighbor index
MEK	methyl ethyl ketone
Om-POSS	octamethyl polyhedral oligomeric silsesquioxane
PMDETA	pentamethyldiethylenetriamine
PGMA	polyglycidylmethacrylate
POSS	polyhedral oligomeric silsesquioxane
PD	partial discharge
PP	polypropylene
SEI	special energy input
TEM	transmission electron microscopy
TGA	thermogravimetric analysis
THF	tetrahydrofuran
XPD	x-ray powder diffraction

CONTENTS

1 INTRODUCTION

Considering our present lifestyle, electricity and its distribution are crucial to human society. Electrical insulation materials, i.e. dielectric materials, are a vital part of the components used in the utilization of electrical energy. The shift from ceramic electric insulating materials and oil-paper insulations to polymeric materials has been a major change in the field of high voltage insulation technology during the past three decades. Today, polymers are widely used in high voltage equipment as they can withstand high voltages. They have high breakdown strength, but their charge storage ability is low and they are not as stable over long periods of time as ceramics are. There has been an attempt to combine ceramic materials into polymers to increase their permittivity or gain better thermal and mechanical properties. However, the breakdown strength of the composites is reduced at high filler concentrations, which are needed to improve permittivity and any potential increase in energy density is lost.[1-3] Polymers also age and that is not easily predicted in applications.[4-8] At the beginning of the century, as nanoparticles came onto the market, there opened a possibility to try adding only small amount of ceramic particles, ranging in size from 1 to 100 nm, into polymer. The idea of these so called nanocomposites was to produce a large interfacial area between the matrix polymer and nanofillers, as the interface can act as a trapping site for electrons and prevent breakdown, or ramp up efficiency of the charge storage ability of dielectric material in an electric field.[9, 10]

The main objective of this work was to improve dielectric properties of polymers used in high voltage capacitors by adding inorganic filler into polymers. Simultaneously the structure of the composites was characterized to understand the features in the structure that determine the functionality of the material. Two types of organic polymers were used as a matrix for different types of inorganic fillers, ranging from molecules to colloidal structures. One matrix is thermoplastic; polypropylene, and it is already used in high voltage capacitors. The other is thermosetting copolymer; epoxy that can be cured at rather low temperatures and it is relatively easy to handle at laboratory scale. As it is a good electric insulator, it can be used as a model system with an en-

semble known as bimodal-polymer-brush-grafted particles and focus the study on the charge layer at the interface between nanoparticles and polymers to see if it has an effect on the dielectric properties, as has been hypothesized. In this composite, silica nanoparticles are grafted with bimodal ligands. A short ligand, oligothiophene or ferrocene, controls the electrical properties and a long epoxy compatible ligand, polyglycidylmethacrylate (PGMA), ensures optimal dispersion.

Various characterization methods were used in an attempt to correlate dielectric properties with the multiscale structure of the nanocomposites. The used methods were transmission electron microscopy (TEM), Raman microscopy, optical microscopy, x-ray powder diffraction (XPD) and computerized x-ray micro-tomography (CXμt).

2 A DIELECTRIC IN ELECTRIC FIELD

Dielectric material does not contain free electrons and becomes polarized when it is placed under an electric field. Our present view of electronic transport in polymeric insulators is based on the energy band theory of crystalline solids. Although polymers are amorphous or microcrystalline and have no long-range order that is characteristic of a single crystal, the atoms are arranged like that of a corresponding crystal. The short-range order is expected to cause some of the features in the electronic properties of the crystalline state: the existence of conduction and valence bands separated by a gap and localized states caused by imperfections. There are also extended states present, i.e. an electron in one of these states is not localized but is free to move through the solid with reasonably good mobility.[11] (see Figure 2.1)

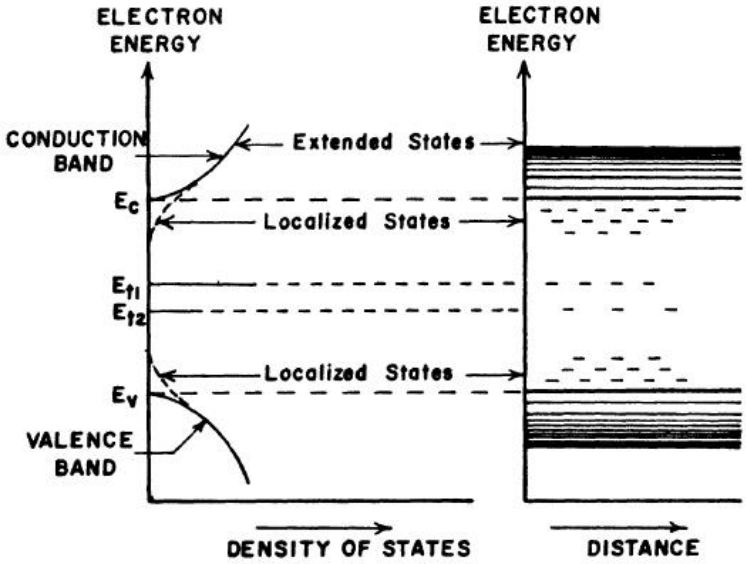

Figure 2.1 Density of electron states as a function of electron energy, and the location of these states through the solid. This image is from reference 11. Copyright ©1975 IEEE

When an electric field is applied to an insulating material, three basic processes can take place: the dipoles tend to rotate, ions migrate and a space charge can be injected at the interfaces, depending on parameters such as temperature or an applied electric field.[12] (see Figure 2.2) Polarization in a dielectric material can be classified into electronic, orientational, atomic or ionic and interfacial polarization. The prevailing temperature and frequency of the applied field will determine what process is triggered. At low frequencies, the polarizability of a material has contributions from all the high

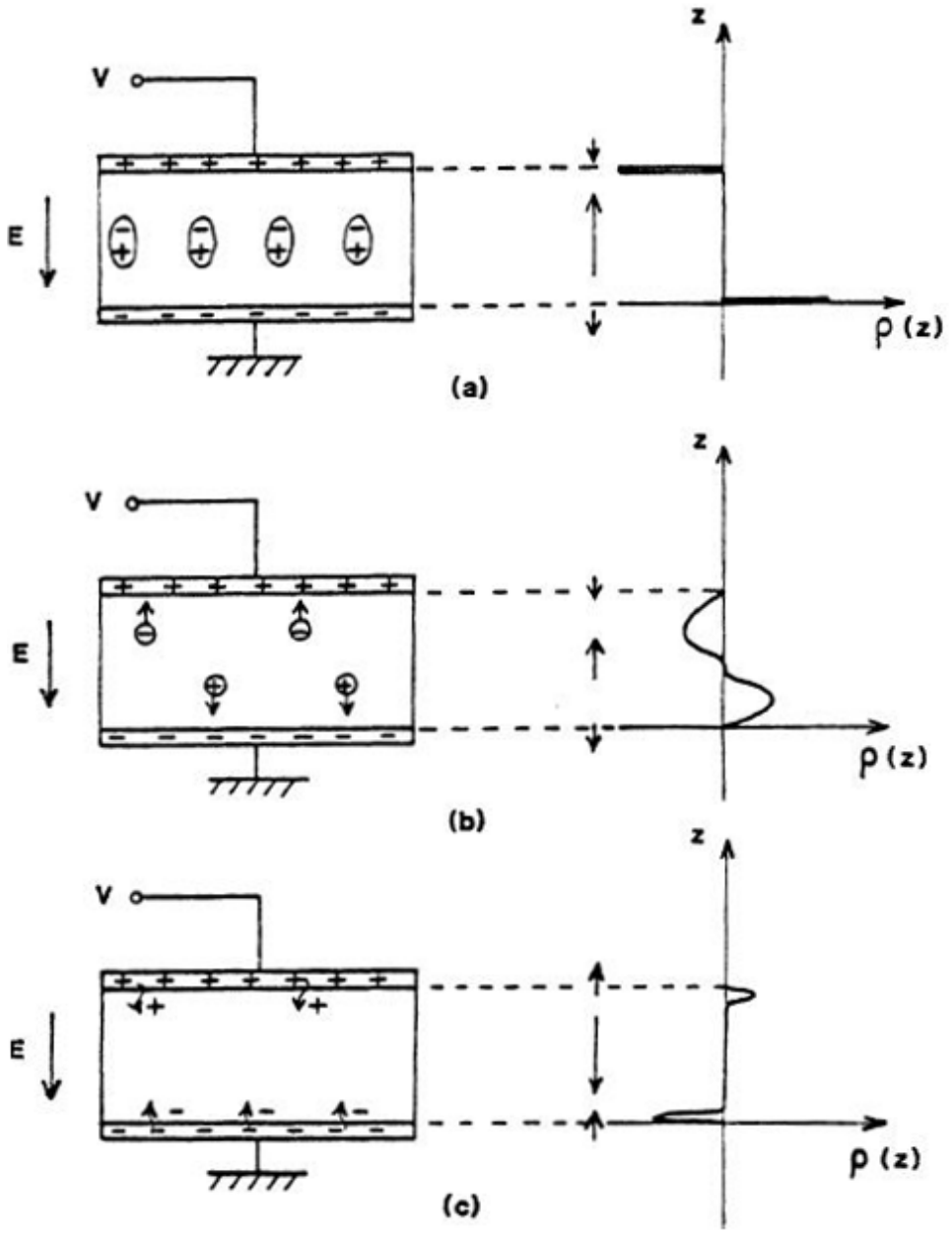

Figure 2.2 Development of a charge distribution p(z) in a dielectric material subjected to an electric field (a) associated with dipole orientation, (b) by ion migration, and (c) by charge transfer at the interfaces. This image is from reference 12. Copyright © 1986 IEEE.

frequency mechanisms that can maintain the speed of an alternating electric field, which results in an increase in the dielectric constant.[13] (see Figure 2.3) The complex dielectric constant ε, that can be divided into real and imaginary parts ε' and ε'', respectively, describes the amount of interaction that the material has with the electric field, also known as electric permittivity. The imaginary part is associated with the amount of energy that is absorbed by the material and is called dielectric loss. Permittivity or dielectric constant are terms used for the real part and are used for all frequencies of the electromagnetic spectrum; for visible light, the term refractive index is commonly used.[14] There is also time required for the polarization to reach its maximum, like a viscous lag. This is called dielectric relaxation and is present when an electric field is applied or removed and must be taken into account when considering frequency variation of permittivity.[15]

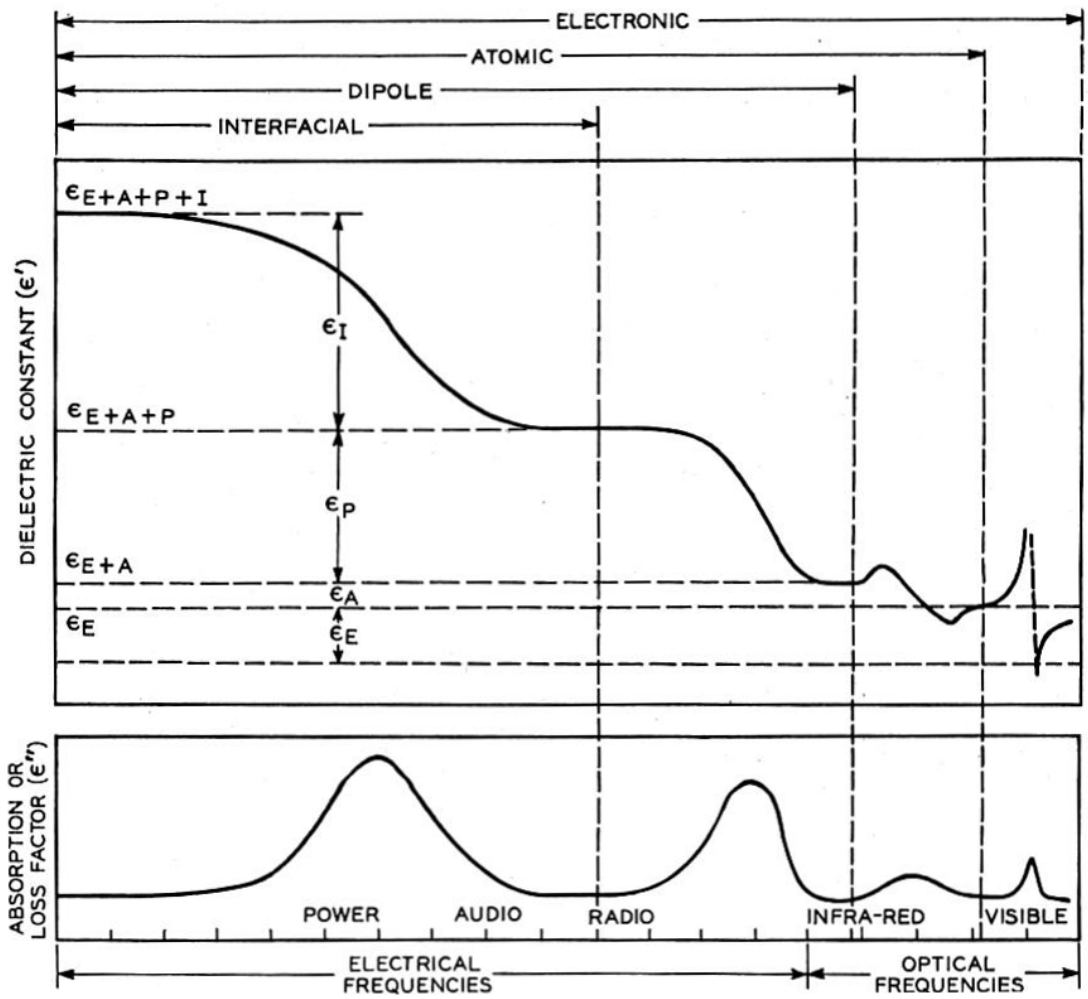

Figure 2.3 Schematic diagram of ε′ and ε″ as a function of frequency. This image is from refence 13. Copyright © 1937 Alcatel-Lucent.

The effects of polarization phenomena can be discussed using electromagnetic theory. One way dielectric polarization at a macroscopic scale is easily illustrated is to place the material between two parallel conducting plates, having area *A* distance *d* apart, and apply a constant potential difference between them; this system is called a capacitor. The capacitance of this system can be measured and it is the property of a capacitor to store charge under an electric field. If edge effects are neglected, the electric field is inversely proportional to the distance between the plates. A charge stored can be represented as an increase of the field compared to the situation without the dielectric material. This system of charges is neutral and possesses a dipole moment:

$$\mu = AE\varepsilon_0(\varepsilon - 1)d \tag{3.1}$$

where $\varepsilon_0$is the electric permittivity of a vacuum.

Induced dielectric polarization can be represented as the dipole moment per unit volume:

$$P = \frac{\mu}{Ad} = E(\varepsilon - 1)\varepsilon_0 \tag{3.2}$$

The term (ε-1) = χ is called susceptibility.[16]

The polarization charges near the interface of the two media make a potential well in which a charge carrier can be trapped (see Figure 2.4). It is important to note that from this electrostatic point of view, electrons and holes both can be trapped in the same region of the medium of lowest susceptibility.[17]

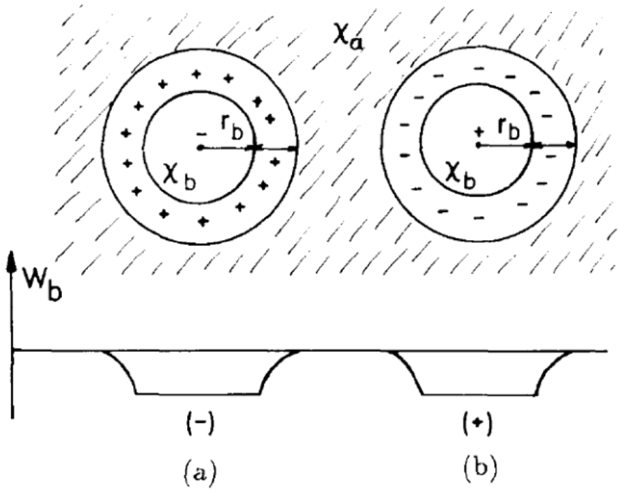

Figure 2.4. Material composed of a medium of susceptibility χ_b smaller than the susceptibility $\chi_a$of the surrounding. Electron trap (a) and positive charge trap (b) inside the region of lower susceptibility due to the polarization charges which appear in the transition region between the two media. W_b is the energy associated with the trapping. This image is from reference 17. Copyright ©1992 IEEE.

For each material under an electric field there is a certain voltage when current starts to increase suddenly, this is known as the breakdown voltage and material is permanently damaged. There is no uniform theory that could explain this phenomenon, and it can be considered to be a sum of different mechanisms. Most current theories relate breakdown to a charge accumulation and displacement of one type or another.[18] Dielectric breakdown is always a thermal process, one way or the other; however, breakdown mechanisms are often still categorized as either an electronic or a thermal breakdown. Breakdown happens rather quickly, usually in ~10 ns in a solid, and is reminiscent of an electron avalanche process that is a well-accepted mechanism for breakdown in gases. Using an electronic breakdown approach, an intrinsic breakdown voltage can be calculated for each material, but solid material cannot survive these kinds of field magnitudes. There is always gas or impurities inside the solid that can cause high local fields in reasonably low voltages, and erosion due to partial discharges can occur, which will eventually erode the whole material. This can be detected from thicker samples as destructed patterns called electrical trees. The geometry of a sample will have an effect on how the breakdown proceeds, or at least how it will be categorized. The electrostatic attraction force between the electrodes can result in an electromechanical breakdown. When it is identified that a material deteriorates chemically due to environmental effects, the mechanism is called electrochemical breakdown. Thermal breakdown is caused by heat generation due to polarization losses and it happens when the material fails to dissipate heat and there is enough thermal energy to release electrons to a conduction band.[16, 19-23]

3 DIELECTRIC NANOCOMPOSITES

Dielectric nanocomposites are dielectric polymeric materials that are doped with small amounts of inorganic particles, with a size of 1 to 100 nm, to produce a large interfacial area between the matrix polymer and the nanofillers and, hence, to tailor the dielectric properties.[24,25] The idea is to use very low amounts of the filler to avoid any percolation. Percolation threshold is a limit of the formation of long-range connectivity in random systems. Below the threshold, particles are not connected to each other. The aim is, for example, to increase the material's dielectric breakdown strength, or the dielectric constant in combination with low loss. It is suggested that nanoparticles could increase breakdown strength by hindering the electrical tree growth within the material.[26,27] There is considerable interest in using these new materials in capacitor applications.[I], 3, 28-31

Currently, there are three major models describing the effect brought on by interfaces.[32] Lewis's model[33] concentrates on electrical properties of interfaces in a way that the particle introduces the interface region to the polymer based on overlapping Gouy-Chapman layers. Louis Georges Gouy and David Chapman introduced a diffuse model of the electrical double layer, in which the electric potential decreases exponentially away from the surface to the fluid bulk.[34, 35] Tsagaropoulos'model[36] tries to explain the chemical and physical features of interfaces based on differences seen on glass transition temperatures and assumes that interfacial regions are formed as the polymer bonds, loosely or tightly, to the particle. Tanaka's multicore model[24] is the most recent and tries to combine these two preceding models.

There are experimental results that suggest that it is not enough just to control the dispersion of particles. In order to improve the charge storage ability of the material, the relative polarity of the particle surface ought to be controlled as well.[37] The added interfacial control, directly bonding the particle to the polymer matrix, can prevent conductive percolation across particle surfaces and increase dielectric breakdown strength.[29] Furthermore, significant reduction in leakage currents and dielectric losses as well as improvement in dielec-

tric breakdown strength has resulted when electropositive, or electronwithdrawing functional groups, were located at the particle surface.[38]

There are several scales that must be considered when trying to elucidate the relationship of structure of nanocomposite to its function: molecular, intermediate and micro-scale. (see Figure 3.1) The local interactions, molecular conformations and the properties of the matrix material need to be considered within the interphase regions. Intriguingly, what still is unanswered is how far interphase regions extend into the matrix and what the properties of these regions are. Also, it should be taken into account whether the interactions that are predicted to occur between the matrix and the nanofiller tend to promote dispersion, or are they even preventing it to happen. Many questions still remain without clarification.[39]

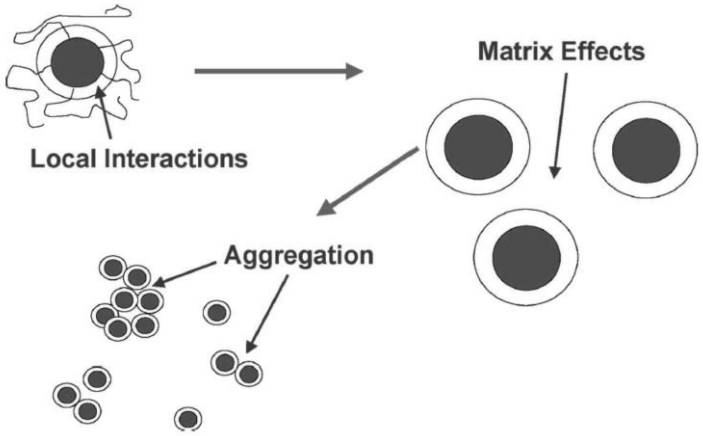

Figure 3.1 Schematic diagram indicating the range of different dimensional levels that need to be considered when attempting to characterize a nanocomposite. This image is from reference 39. Copyright ©2008 IEEE

Nanoparticles can be used in both cross-linked thermosetting polymers and in semi-crystalline thermoplastics. Potentially, when using thermoplastics that are recyclable, it is possible to achieve more applicable and economical insulation structures.[40] The heterogeneous nature of the composition of these polymer nanocomposites brings challenges and requires the development of processing methods[10] and characterization; in practice, it is difficult to assign morphology to an increase in DBS.[41] Also, relatively high filler loadings, such as 10 wt-% TiO_2 particles in epoxy, are reported to be optimal in order to gain good dielectric breakdown strength.[42] To develop these new materials for industrial use, a fundamental understanding of dielectric properties at the nanoscale level is of great importance. There are many ways to mix particles to the matrix polymer. Nanoparticles are usually coated with polar or non-polar organic molecules to make their surface more compatible with the matrix. It was found that dry mixing of these coated particles is problematic; once nanoparticles are dried, they inevitably agglomerate and become very difficult to disperse as they have a very high surface to volume ratio. The harsh mixing condi-

tions needed to redisperse the nanoparticles may degrade the properties of the matrix polymer. [43-50]

In the following chapters, the components of composites used in this study are presented. The used nanofillers range from molecular to colloidal, and surface treatments used are either surfactant or covalent modification.

3.1 Melt compounding: polypropylene (PP)

Polypropylene is a mildly polar hydrocarbon and identical macromolecules of it do not exist.[51] It is semi-crystalline consisting of lamellaes that form birefringent spherulites that grow until they touch another spherulite. Spherulites are aggregates of crystals with a radial fibrillar structure.[52-54] (see Figure 3.2) Three different crystalline phases are found to exist in PP depending on the crystallization conditions used: α (monoclinic), β (hexagonal), γ (orthorhombic).[55, 56] Polymer crystallization has been studied since the 1960s, and yet no molecular theory exists. It is controversial whether preordering occurs before the onset of crystallization or not.[57] Partially crystalline polymers have both a glass transition state and a melting point. Below glass transition temperature, molecular motion is restricted to the rotation of side groups or their parts.[16]

Thermoplastic polymer composites are processed physically using extrusion. Using this approach, good dispersion of the filler can be achieved, as polymer gains increased mobility through the input of thermal energy, and the nanofillers are mechanically dispersed and mixed under the influence of shear forces. When the effect of processing conditions was studied, it was noticed that a specific energy input (SEI) is related to the shear intensity, which correlates closely to the degree of mixing.[58] Small crystal size and low defect amounts are related to improved DBS of PP.[59] There is still a need for resolving the connection between the morphology of PP and its DBS.[60]

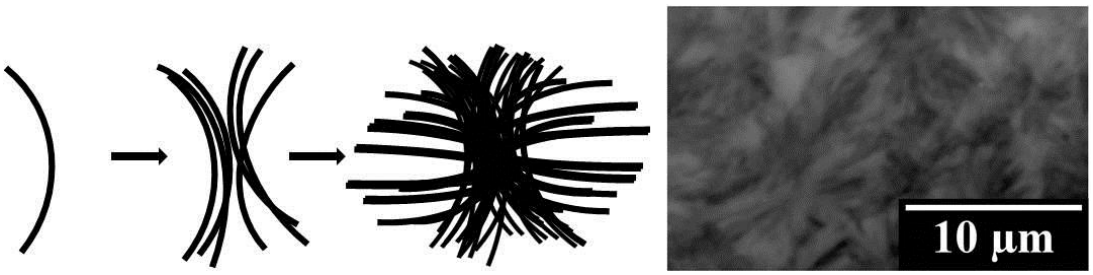

Figure 3.2 Stages in the formation of a spherulite from a stack of lamellae; a side view and TEM micrograph of spherulites; a top view.

3.1.1 Molecular filler: octamethyl polyhedral silsesquioxane (Om-POSS)

Cage-like silsesquioxanes are usually called polyhedral oligo-silsesquioxanes or polyhedral oligomeric silsesquioxanes (POSS). Interest in these molecules has been increasing since the early 1990s, and attempts have been made to try to understand the structure-property relationship of the molecules blended into polymers.[61] This class of highly symmetric molecules usually features a nanoscopic size, approximately 1.5 nm in diameter when the vertex (R) groups are included. These molecules have a hybrid inorganic core/organic shell structure (see Figure 3.3) They can be regarded as the smallest possible silica particles. POSS-based materials, including fire retardants, biomaterials, dielectric materials, organic light-emitting diodes, lithography resists, catalysts, membrane fuel cells and battery membranes have recently been introduced.[62-64]

Octamethyl POSS (Om-POSS) is a molecule that has methyl vertex groups. It is a non-reactive, crystalline solid. Physical mixing is believed to be an efficient method to disperse POSS in the polymer matrix mediated by van der Waals or hydrogen-bonding interactions.[65] However, proof of molecular level dispersion has not been reported using this mixing approach; instead, there is evidence for strong particle-particle interactions.[66] Additionally, it has been reported that in PP, om-POSS acts as a nucleating agent and is mixed mainly as microcrystals.[66-68] It must be taken into account when processing om-POSS that it sublimes at elevated temperatures (>200°C) under a nitrogen atmosphere.[69, 70] Phase changes inside the polymer is a probable cause for observations of the average crystal size of om-POSS decreasing as it is mixed into the polymer matrix.[71] The om-POSS as a filler in PP has the ability to increase the dielectric breakdown strength of PP[72] and epoxy.[73]

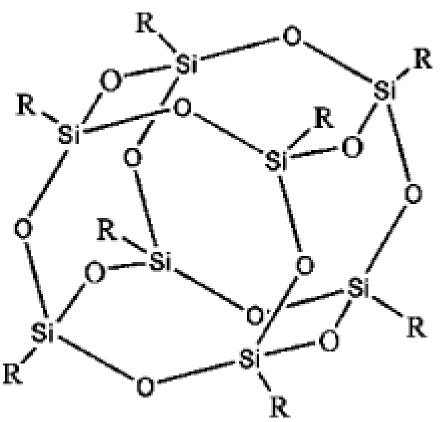

Figure 3.3 Chemical structure of om-POSS molecular nanofiller. This image is from reference 71. Copyright © 2007 Wiley Periodicals, Inc.

3.1.2 **Crystalline filler: surfactant coated nano-$CaCO_3$**

Synthetic, so-called precipitated calcium carbonate is commonly produced by a recarbonizing process in which natural calcium carbonate is decomposed to calcium oxide and carbon dioxide. Calcium oxide with water forms calcium hydroxide that reacts with carbon dioxide and as a result pure, synthetic calcium carbonate precipitates.[74] It is commonly used in large mixture ratios to reinforce polypropylene.[75] The improved toughness is related to the β-nucleating effect of $CaCO_3$ and the increase in crystallinity of PP.[76-79] It is well excepted that improvements in mechanical properties are related to good dispersion of the filler[80, 81] The β-nucleation efficiency and matrix interactions are dependent on the surface treatment of the particles; it has a crucial role in determining the properties of the composite.[82-92] When considering the composite processing, aggregated nano-$CaCO_3$ causes anisotropic polymer chain orientation in extrusion[93] and introduces porosity into PP films under biaxial stretching.[94] This is detrimental to the application. Dielectric breakdown strength of neat polypropylene is reported to decrease if it contains 0.1-1.0 nm diameter voids.[95] $CaCO_3$ hardly affects the flammability of PP, [96] but it is found to increase its thermal conduction.[97]

There are only a few studies of the dielectric properties of $CaCO_3$ polymer composites and the increase of permittivity and losses of composites are explained by the moisture absorbed by $CaCO_3$.[98] The loading of 3 wt-% of the surfactant modified $CaCO_3$ in PP has not shown any increase of permittivity.[99] For $CaCO_3$ filled PP composites, a raised AC breakdown strength has been reported.[100] Dielectric spectroscopy measurements have shown that the smaller particle size raises the permittivity compared to pure continuous $CaCO_3$ at low frequencies.[101]

3.1.3 **Amorphous filler: surface modified fumed silica**

Fumed silica, also known as pyrogenic silica as it is produced in a flame, can have a very small particle size (2 nm) and if properly dispersed would provide a very high surface/volume ratio and large interfacial volume. It is also a cheap alternative as a filler for possible up-scaled application.[102] Silica is an excellent electrical insulator. Amorphous silica has been studied to see whether it can act as an electron trap under electron bombardment.[103] Fumed silica decreases the size of spherulites and the crystallinity of PP in nanocomposites.[104] Silica has been mixed into polymers together with other fillers.[105, 106] Even considerable improvements in voltage endurance of polymers filled with fumed silica have been reported[106, 107, [I]] For example, 12.5 wt-% vinylsilane-treated fumed silica has improved the voltage endurance of cross-linked polyethylene, a composite useful for cable applications. For this particular material, the degree of crystallinity was claimed not to be a predominant factor in increasing breakdown strength and the highest voltage endurance was achieved for composites believed to have a covalent bonding between the matrix and the filler.[108] Below 10 wt-% fumed silica in biaxially oriented blown PP films have shown

breakdown strength, energy density, corona resistance and mechanical properties such as impact strength, tensile strength and ductility comparable to or superior to blown films of the un-filled polymer composition.[28] There are, however, no indications that fumed silica would have considerably improved the permittivity of the polymer composites.

3.2 In Situ polymerization: Epoxy

Epoxy is the most abundant thermosetting polymer. It is highly cross linked, glassy and brittle at room temperature. The reaction between an epoxy resin and a hardener is an irreversible exothermic poly-addition, i.e. no by-products are formed, and the epoxy plastic cannot be decomposed into epoxy resin and hardener. There are more than 50 different substances that fulfill the definition for an epoxy resin. The epoxies are versatile as there are several hundred different hardeners available. [109, 110] Thermosetting composites with epoxy are made by in situ polymerization.[111] (see Figure 3.4) If the nanofiller can be mixed with the resin in a non-dried form, it is better for particle dispersion; however, particles that solvate to solution are not necessarily compatible with the matrix, and the solvent might also deteriorate the matrix polymer or introduce undesirable ions to the composite.

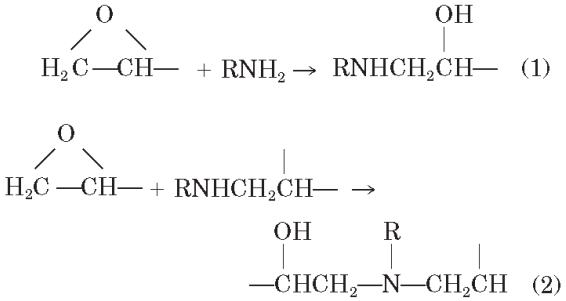

Figure 3.4 Typical curing, i.e. cross-linking reactions, of epoxy resin using an aliphatic diamine curing agent below 150°C. This image is from reference 111. Copyright © 1999 John Wiley & Sons, Inc.

3.2.1 Colloidal filler with electro active surface: bimodal-polymer-brush-grafted silica

A polymer brush is simply a polymer chain tethered to a surface. They have been studied for over 30 years. There are two methods used to produce these brushes: the “grafting to" approach, where chains are polymerized and subsequently attached to the surface, and a “grafting from" approach, used where polymerization takes place from a site on the surface of a particle. The

latter has the advantage of achieving higher graft densities since previously grafted chains do not inhibit the attachment of additional chains. “Grafting to”, used in this study, is quick and easier to scale up and provide some flexibility in the chemistry of the attached molecule.[112] The limitation is in the lack of control over graft density, but good dispersion of particles has been modeled using this approach,[113] and a phase diagram has been experimentally validated to predict the dispersion for bimodal-polymer-brush-grafted nanoparticles.[114] “Grafting to” can be done using so called “click” chemistry,[115, 116] where the idea is that it has a high thermodynamic driving force. This type of reaction proceeds rapidly to completion and also tends to be highly selective for a single product. The analogy would be a spring loaded for a single trajectory.[117] This approach has been reported for functionalization of silica[118-122] and also used as a way to make so called “matrix free” silica polymer composite by using alkyne and azide modified polymer brushes on silica.[123] PGMA has been used for dispersing high loadings of TiO_2 to epoxy with a high refractive index and transparency.[124] Electro-active alkyne terminated oligoaniline has been previously attached to polymers on silica particle surfaces retaining its electro-activity. [125]

4 EXPERIMENTAL METHODS

4.1 Nanoparticle surface coating and composite processing

The filler materials used in this study were om-POSS, $CaCO_3$ and SiO_2. Om-POSS was used without any surface functionalization with an average crystal size of 170 nm. $CaCO_3$ was precipitated as 60 nm particles with stearic acid as a surface coating. In PP, SiO_2 was 12 nm fumed silica with a hydrophobic surface. In epoxy systems, SiO_2 was added as a solution of 15 nm colloidal particles with bimodal-grafted-brushes tethered on the surface. This ensured a high density of short chains with tailored dielectric behavior, and a low density of long chains that are compatible with the matrix. The PP composites were mixed using extrusion. First PP and the filler were premixed in dry form and subsequently melt mixed. The epoxy composites were mixed in shear mixer, degassed and cured in silicone molds for 10 h in room temperature followed by 10 h in 60°C and finally 4 h in 100°C.

4.1.1 **Bimodal-polymer-brush-grafted silica**

Silica particles were modified using copper(I)-catalyzed Huisgen 1,3-dipolar cycloaddition of azides and terminal alkynes, [3+2] cycloaddition (CuAAC) reaction.[126]

A suspension (40 ml) of 30 wt-% colloidal silica particles was added by funnel into a dried 250 ml two-necked, round-bottom flask with 3-(Chloropropyl)-trimethoxysilane (1.18 g, 6.0 mmol) and dried THF (40 ml, 72 h over a molecular sieve). The reaction mixture was refluxed in 100°C oil bath under an argon balloon overnight and then cooled to room temperature. The reaction mixture was precipitated into a large amount of hexanes (500 ml). The particles were recovered by centrifugation at 3000 rpm for 15 min. The particles were then dissolved in 20 ml of acetone and precipitated in 200 ml of hexanes. The functionalized particles were dispersed directly into 50 ml of DMF for subsequent use. An aliquot of the functionalized silica nanoparticles was dried and

subjected to thermal gravimetric analysis to determine the amount of silane agent anchored onto the particles.[127]

3-(Chloropropyl)trimethoxysilane functionalized silica particles (<0.59 g (3 mmol)) and sodium azide (<0.3 g, 5.52 mmol) were added into 100 ml round bottom flask in DMF and refluxed in 100°C oil bath for 4 h. After the reaction, excess sodium azide was washed with deionized water three times. The particles were dissolved in THF to form a clear solution. An aliquot of TGA was taken (weight loss due to linker was 5-6%) and concentration was determined (mg/ml).

0.04 g ethynylferrocene or 0.08 g alkyne terminated oligothiophene [1 equiv] and 0.2 g alkyne terminated PGMA [1:10 equiv], (see Figure 4.1) 0.8 g functionalized particles; azide [1 equiv], and PMDETA (40 µL [0.5 equiv]) was added in 40 ml of THF. The mixture was degassed by bubbling argon gas for 5 min to get rid of oxygen before adding CuBr (approx. 14 mg [0.5 equiv]). CuBr was purified with glacial acetic acid and washed in ethanol before use, bubbled with argon gas for additional 5 min, and then stirred for 24 h. Particles were precipitated by methanol and centrifugation (4000 x g 10 min) and then mixed into bisphenol-A based epoxy resin and solvent residue was evaporated before adding the aliphatic amine based hardener.

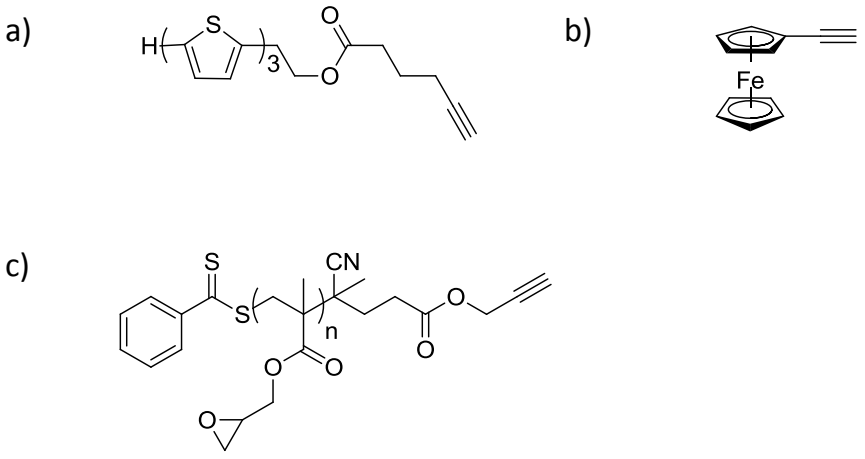

Figure 4.1 Chemical structures of entities tethered on the silica surface by click reaction: a) alkyne terminated oligothiophene b) ethynylferrocene c) alkyne terminated PGMA

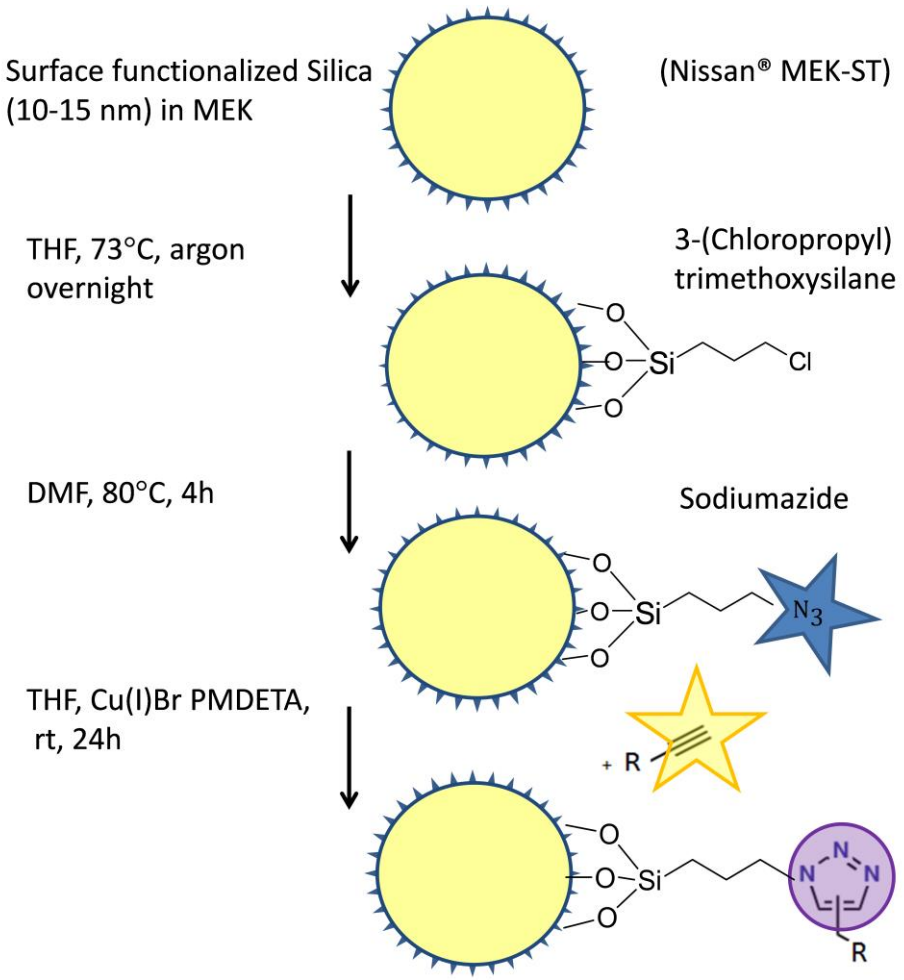

Figure 4.1 Surface modification process of silica to supply bimodal brush grafted core functionalized nanoparticles**.** Colors indicate the reactive parts and product of used grafting to "click" reaction.

Functionalized silica was analyzed with TGA, infrared spectroscopy (IR) and UV-vis spectroscopy after each processing step. (see Figure 4.1) Attachment of each linker to particles was detected by IR: PGMA can be confirmed from a C=O vibration at 1733 cm^{-1} and a characteristic peak of an azide group is seen around 2100 cm^{-1}. The completion of "click"reaction was verified by the disappearance of the azide peak. Attachment of electroactive molecule was verified by UV-vis spectroscopy: oligothiophene at 360 nm and ferrocene at 440 nm. The grafting density σ was calculated from the weight loss ratio determined by TGA: [128]

$$\frac{z}{(1-z)} = \frac{w_{polymer}}{w_{silica}} = \frac{w_{polymer}}{\rho N \frac{4}{3}\pi r^3} \tag{4.1}$$

The grafting density σ is simply number of entities grafted onto silica particles: the number of grafted chains ($w_{polymer}N_A/M_n$) is divided by the surface area of colloidal silica ($4\pi r^2N$). silica (chains/nm^2):

$$\sigma = \frac{w_{polymer}\, N_A/M_n}{4\pi r^2 N} = \frac{r\rho z \times 10^{-21} N_A}{3(1\text{-}z)M_n} \tag{4.2}$$

where w, N_A, N and z are the weight, Avogadro's number, the number of particles and weight loss of polymer chains respectively. Residue weight (1-z) is the fraction of silica. Supposing that the SiO_2 particles are spherical with a radius r of 7.5 nm and density ρ of 2.2 g/cm^3 for amorphous quartz, and the molecular weight of the polymer M_n was 15000 g/mol; the grafting density of PGMA was estimated to be between 0.02-0.05 polymer chains/nm^2. When both a short and long brush was attached simultaneously, the estimation of achieved grafting density could be determined since oligothiophene decomposes right after 250°C and PGMA decomposes after 400°C.

4.2 Structural characterization

There are two scales to be considered, micro and nano, if the dispersion of fillers in original structure of PP composites was to be illustrated. Mostly, the structural characterization was done using two techniques: Raman microscopy and TEM. Two kinds of samples were used: cast film samples that have an approximate thickness of 500 µm and biaxially oriented films with a thickness of around 20 µm, called oriented samples.

4.2.1 **Raman imaging**

For the Raman analysis of cast film samples, a dispersive micro-Raman spectrometer (Bruker Senterra R200-785) equipped with a linearly polarized diode laser (785 nm) in back-scattering geometry was used.

For confocal imaging of om-POSS composite, the pinhole used was 25 µm with a 100x objective (NA 0.90). The laser power was kept low to avoid overheating the sample (25 mW). At each point, the measurement time was 10 s. The area of interest in the sample was scanned with a motorized stage of 0.1 µm accuracy in two or three dimensions using 0.5 µm steps.

For coarse imaging of $CaCO_3$ composites, the laser power was 100 mW and a slit width of 50 x 1000 µm was used with a 50 x objective in order to get a good signal from larger area. This way, it could be determined whether the dis-

persion of nano-$CaCO_3$ is homogeneous over large areas (~200 μm). The area of interest in the sample was scanned with a motorized stage with 0.1 μm accuracy in two dimensions, using a 3 μm step size. The spectra of composites were measured from a 210 x 210 μm^2 area. Four areas of each sample were then scanned and visualized as an intensity contour plot of a selected characteristic Raman peak of $CaCO_3$ and PP. The PP signal was used as a reference to check that the overall signal level was stable over the measured area. The analysis was done for a PP composite sample series containing 1.8 to 8.1 wt% nano-$CaCO_3$. Altogether, there were samples of eight different nano-$CaCO_3$ concentrations. Pure PP, processed similarly as the composites, was used as a reference. Both cast and oriented film samples were characterized.

4.2.2 **Transmission electron microscopy**

TEM analysis can be used to analyze both micro-and nanoscale particles. This method is the preferred method for nanoscale dispersion studies in cast films. The PP composites are quite soft materials and, therefore, it is challenging to obtain good quality, ultrathin sections for TEM imaging. Especially, the contrast of silica nanoparticles with respect to the PP matrix is also a limiting factor for quantitative TEM analysis. On the other hand, the microcrystallinity of PP can be used as an internal standard to ensure that the structure studied is really in original form. The quality of thin sections has been the limiting factor in acquiring good quality images. For TEM analysis, ultrathin sections of the cast film samples or epoxy blocks were obtained using a Diatome 35° diamond knife at room temperature with a Leica Reichert Ultracut ultramicrotome. The 50-90 nm thick sections were collected on a 400 mesh copper grid and imaged with JEOL-JEM-1200EX or 1400 electron microscope with 2.5 - 75 k magnification. Statistical analysis was performed using images that were converted to a binary format. For PP composites, the particle area and center of mass were determined using the ImageJ®program. Microparticles were excluded from this analysis. The data was further processed to emphasize the distribution of the filler material in the matrix media; the relative volume of the agglomerates was estimated assuming that they are spherical objects. (see Figure 4.2)

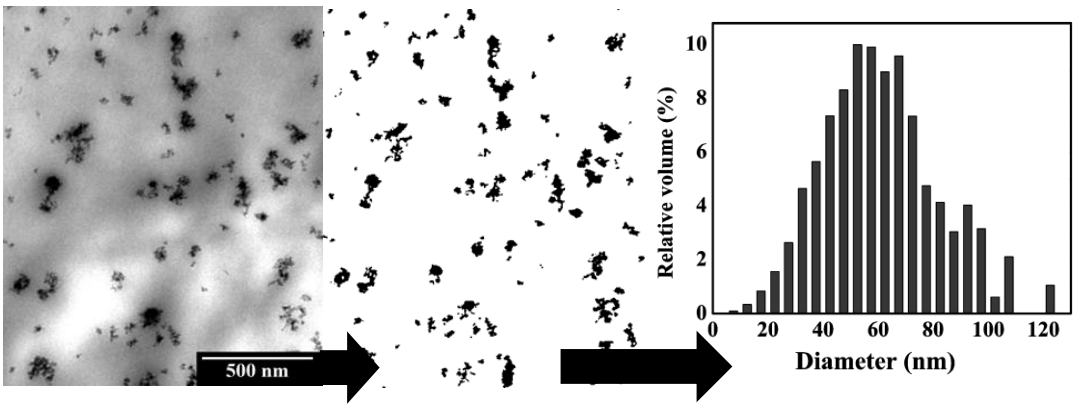

Figure 4.2. Image analysis path to determine average agglomerate size of the filler.

Dispersion quantification was performed for PP composites using two methods with numerical descriptor: the quadrat method (skewness), which measures the uniformity of the spacing of particles and agglomerates, and the 1st nearest neighbor index (NNI), which indicates how well individual particles are separated from one another. These two methods are all relatively insensitive to volume fraction of filler and primary particle size since clusters are treated as point objects and they can be considered to give a value of the quality of dispersion.

The quadrat method divides the sample into cells, counts the number of particles in each cell and reports the skewness of the particle distribution:

$$\frac{\mathrm{N}}{(\mathrm{N}-1)(\mathrm{N}-2)}\sum_{\mathrm{i}=1}^{\mathrm{N}}\frac{(\mathrm{x}_i-\bar{\mathrm{x}})^3}{\sigma} \tag{4.2}$$

where x_i denotes the number of particles in the i^{th} quadrat, $\bar{x}$ is the mean of x_i (i =1,2,…,N), and σ is the standard deviation of x_i. Skewness evaluates the asymmetry of distribution. When counting particles in quadrats, the size of the quadrat was selected to be two times the average diameter of agglomerates, as is commonly used.[130] When a reasonable size is selected for the quadrats, the number of particles tends to be the same in each quadrat when the particles are well mixed, resulting in a skewness that is close to zero. Aggregates will result in a large number of empty or less populated quadrats and skewness will be then non-zero. The higher the deviation is from zero, the poorer the dispersion.

In the NNI analysis, each agglomerate or particle is treated as one body, and the mean distance to the closest agglomerate or particle $\langle L_n \rangle$ is compared to the distance expected for an equilibrium distribution $\langle R_n \rangle$ of particles having the same diameter and volume fraction.[131] NNI is simply the average of the actual closest neighbor distances divided by the randomly distributed case:

$$\mathrm{NNI} = \frac{\langle L_n \rangle}{\langle R_n \rangle} \tag{4.3}$$

NNI >1 indicates regularity and <1 indicates clustering.[132] In previous studies of nanodielectrics NNI values of >0.7 and a low absolute value of skewness (<1.5) are related to improved DBS.[129]

For epoxy composites, using MATLAB®, free-space length L_f was used to quantify dispersion from binary images. The free-space length is defined as the width of the largest randomly placed square for which the most probable number of intersecting particles is zero. This parameter is well-suited for comparing different loadings as the measurement is physical quantity; the distance between particles. But it is not relative to random dispersion as for example NNI is. For the same filler loading, the further the dispersion is from uniform, the longer the L_f becomes (see Figure 4.3). The code was retrieved and used according to the literature.[133, 134]

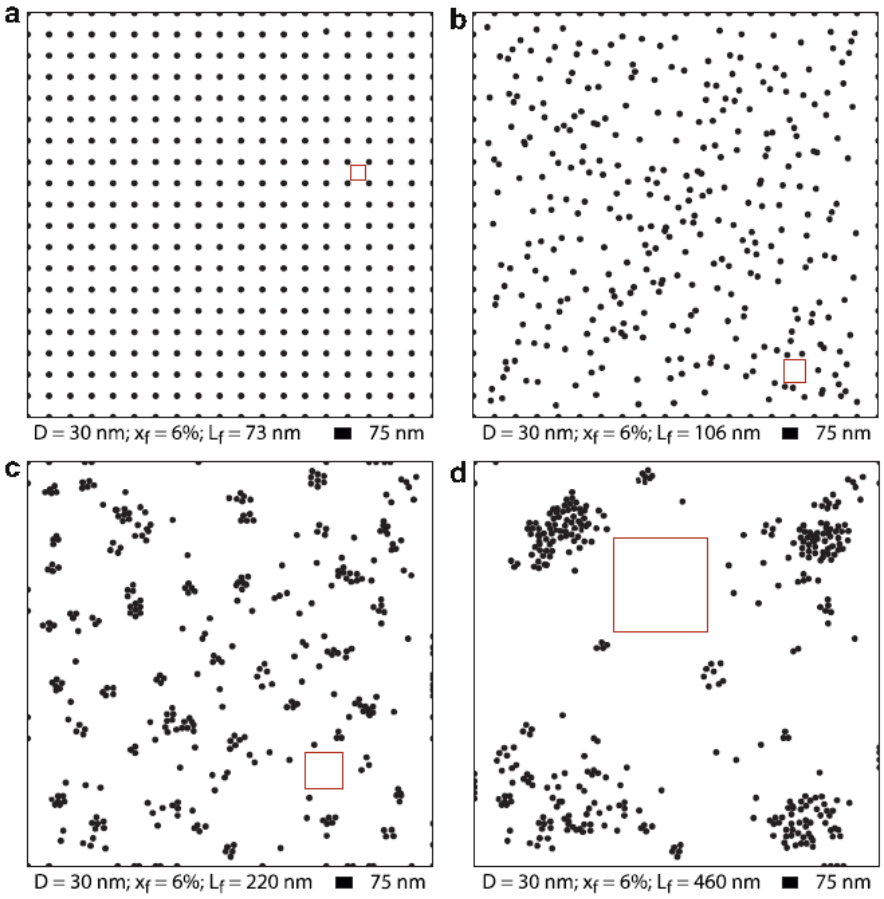

Figure 4.3 Varying dispersions of 30 nm particles at 6% loading a) uniform dispersion L_f= 73 nm; b) random dispersion L_f =106 nm; c) clustered dispersion L_f = 220 nm; d) agglomerated dispersion L_f = 460 nm. Open squares have a length equal to the free-space length which increases as the dispersion worsens. This image is from reference 131.

4.2.3 Other methods

As there were high density differences between filler particles and the matrix, computerized X-ray micro-tomography (CXμT) could be used to study the micron-scale 3D structure of composites. The resolution of the technique is 0.9 μm. CXμT techniques, based on synchrotron radiation sources, have been used in probing the internal 3D structure of materials for decades. The method has become more feasible as table-top tomographic scanners utilizing x-ray tubes become available. Although such scanning techniques were initially developed for the medical field at a macro-level, they are increasingly being adopted in various research sectors on microstructure analysis.[135, 136] In CXμT, a 3D image of the sample is calculated from the transmission or reflection data collected by illuminating the object from many different directions. The scanner uses a continuous incoherent x-ray beam to produce 2D shadowgraphs from multiple angles. Reconstruction of the shadowgraphs produces cross-sectional images of the absorption coefficients of the x-ray beam.

For describing the average crystallite size of the constituents, powder x-ray diffraction was used. The average crystallite sizes of PP and fillers were estimated using the simple Scherrer method that gives the average crystal size of the crystallites in direction normal to the lattice planes. The method is based on the broadening of diffraction peak profiles as a function of decreasing size of the diffracting crystals.

4.3 Dielectric properties

4.3.1 Dielectric breakdown strength (DBS)

The DC breakdown strength is a very important feature and, therefore, was measured from all the composite samples. It was measured for PP from biaxially oriented films and for epoxy composites it was measured from recessed samples to gain quasi-uniform electric field.[137] In oriented film, PP sample breakdown results were fitted with a 2-parameter Weibull distribution, whose cumulative distribution function is given by

$$F(\mathrm{x}) = 1 - \exp\left\{-\left(\frac{\mathrm{x}}{\alpha}\right)^{\beta}\right\} \tag{4.4}$$

where F(x) is the probability of breakdown at a certain electric field strength x (kV/mm). The scale parameter α is related to the 63.2% probability of breakdown at field strength α, and the shape parameter β describes the shape of the distribution. The higher the value of β, the narrower the spread of indi-

vidual breakdown strength results are. The β is also known as shape factor. The shape of the distribution and deviation between parallel samples for each composite can be visualized by percentiles, corresponding to the probability of breakdown at the respective electric field magnitude.[138, 139]

When recessed epoxy samples were analyzed, 3-parameter Weibull distribution was found to fit the results better.

$$F(\mathrm{x}) = 1 - \exp\left\{-\left(\frac{\mathrm{x}-\mathrm{t}}{\alpha}\right)^{\beta}\right\} \tag{4.5}$$

This three parameter Weibull is commonly used in failure analysis.[140] There is an obvious threshold value, t, required for breakdown to happen.

4.3.2 **Dielectric spectroscopy**

Dielectric permittivity and loss factor of the materials were determined by measuring the complex impedance of the samples. The real and imaginary parts of the complex permittivity (ε' and ε") and relative complex permittivity (ε_r) were calculated from the measured parallel capacitance and resistance:

$$\varepsilon' = \left(\frac{\mathrm{C_P} - \mathrm{C_e}}{\mathrm{C_0}}\right); \mathrm{C_0} = \frac{\varepsilon_0 \mathrm{A}}{\mathrm{d}} \tag{4.6}$$

$$\varepsilon'' = \varepsilon' \tan\delta = \frac{\varepsilon'}{2\pi \mathrm{R_P C_P f}} \tag{4.7}$$

where C_P and R_P, respectively, are the measured parallel capacitance and resistance at frequency f, and C_e is the error capacitance due to small electric field distortions at the electrode edges.[141] C_0 is the vacuum (geometric) capacitance defined by electrode area A, ε_0 is the permittivity of a vacuum, d is the average thickness of the sample, and tan δ is the dielectric loss tangent.

5. RESULTS AND DISCUSSION

Studies of nanodielectrics rarely concentrate on structure, as it is challenging to determine properly. Vast parts of the literature also lack understanding about the interfacial effect. Results published seem to vary tremendously, and all findings must be restricted to each composite in question. There seems only a little dependence of the improvement of properties on nanoparticle concentration. This can be explained by difficulty of mixing particles with high surface energy evenly into the polymer matrix, as particles will form agglomerates and the interfacial area decreases. It is also difficult to study one particular property of dielectric material as the results can be dependent on sample preparation, rather than properties of the material itself. Also, the precursors are commercially made and their whole content is often not revealed entirely. For possible future applications, it is still important to understand the detailed composition of the material in order to avoid possible drawbacks caused by microparticles formed from possibly agglomerated nanoparticles. According to structural characterization done in this work; it seems that reason why poorly dispersed nanoparticles still improve the dielectric properties of the polymer is the increase in the stability of the composite caused by structural changes that the filler imposes on the composition and structure of the polymer. But what is also found out is when the filler is truly dispersed at nanoscale, it seems that the increased polarizability introduced by nanofiller, plays a major role in improving the dielectric properties of the material.

5.1 PP composites

This section briefly describes the main results of the work presented in Publications I-III. The main motivation for these studies was to perform structural characterization of various composites and correlate that information to dielectric properties in order to gain insight into the structure-function relation-

ship. Challenging for the structure property relations of these materials were that the DBS level of reference material was quite low compared to values for different industrial PP capacitor films[142] indicating that there might be some other effects than caused by fillers, that are also important for gaining preferred material properties.

5.1.1 Molecular filler: om-POSS

The molecular filler om-POSS was found to be dispersed in PP mainly as agglomerates formed from nanocrystallites (see Figure 5.1) From CXμT, the concentration of om-POSS at the microscale was estimated at 2.3 wt-%, as the added amount of om-POSS was 3 wt-%, so only a small portion from the added filler was properly dispersed as nanoparticles. Microagglomerates were found to be elongated and evenly distributed in the matrix. (see Figure 5.1b) The diameter distribution extends from about 1 μm to 16 μm and the most probable diameter is approximately 6 μm.

Crystal agglomerates of om-POSS were formed when the PP melt was cooled, as the average crystallite size determined from powder x-ray diffraction (XPD) was unexpectedly diminished during processing, from 170 nm to 40 nm, apparently due to om-POSS sublimation-condensation phase transition during melt mixing at ~200°C. TEM reveals that there is also the polymer seen inside these crystal structures. (see Figure 5.2a) The XPD patterns are presented in Figure 5.2b. Based on the XPD pattern of PP, the crystalline zones in a sample are mainly in an α-crystal phase. However, at least one weak diffraction peak at ~16.0° 2θ is observed only in PP sample, which indicates the presence of a low fraction of the β-phase which is missing from composite, so the addition of om-POSS will create differences in the microstructure of PP.

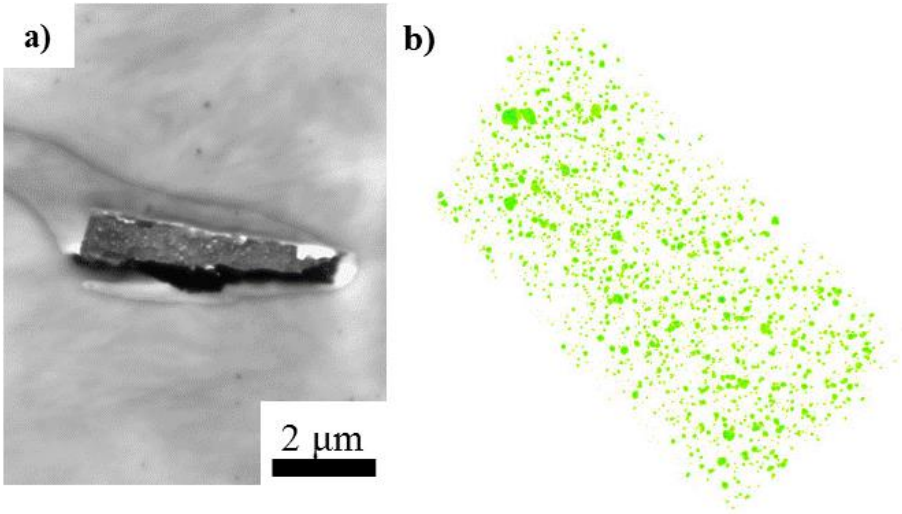

Figure 5.1 Dispersion in 3 wt-% om-POSS PP composite: a) TEM image and b) CXµT visualization of the the particle phase. Physical dimensions of the sample are (1.760 x 0.813 x 0.339) mm. (CXµT courtesy of Viivi Nuottajärvi)

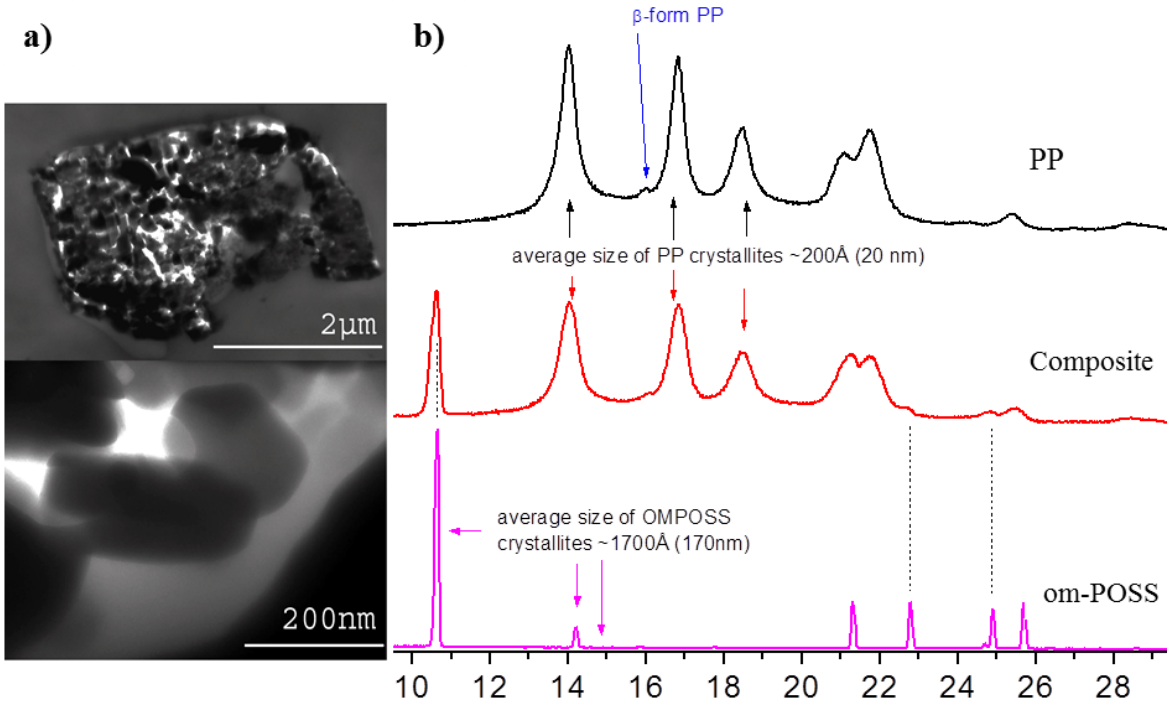

Figure 5.2 a) TEM images of an om-POSS particle in composite sample. It can be seen how the polymer material has intruded the om-POSS microcrystal. b) XPD patterns of PP, om-POSS-PP composite and om-POSS powder samples. Diffraction peaks used for crystallite size evaluation are indicated by arrows. The average crystallite size of om-POSS in the composite is 40 nm; showing that in the fabrication process a dramatic reduction of the crystallite size takes place. (XPD patterns courtesy of Manu Lahtinen.)

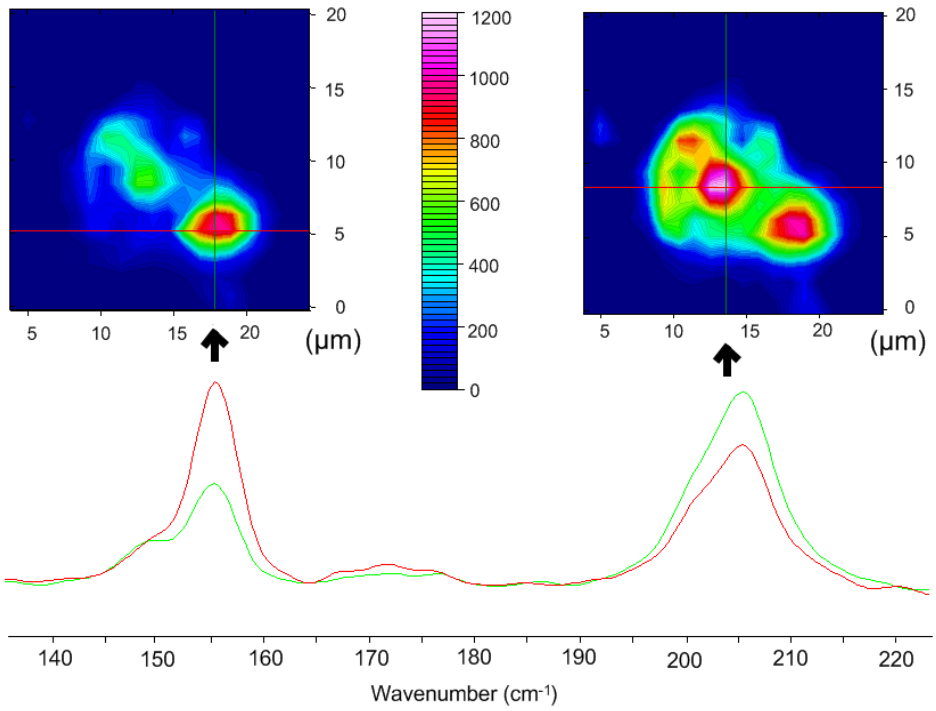

Figure 5.3 Raman intensity contour plots of an om-POSS particle in a composite generated by integrating intensity of the peak at 157 cm^{-1} (left image) and at 206 cm^{-1} (right image). The crosses situated in the intense regions of the contour plots mark the place where the spectra below are collected. The difference in the images reflects the relative difference of the peak intensities in different regions of the agglomerate. This image is from Publication II.

In the confocal Raman studies, it was noticed that relative intensities of the characteristic peaks vary depending on the measurement spot (see Figure 5.3). If different crystals were experimentally measured with changing the polarization of laser and the analyzer; phenomena was further emphasized, and the peak intensities varied tremendously when polarization was changed. (see Figure 5.4a) But, if the measurement volume was increased, the relative peak intensities approached constant value. The theoretical DFT calculations were done by Abinit-code by changing the crystal orientation, in a linearly polarized electric field, and they showed qualitatively similar changes in relative peak intensities.[II] (see Figure 5.4b) A plausible explanation of this effect is the orientation of the crystallites in agglomerates. The tensorial nature of Raman scattering leads to a dependence of the signal intensity on the relative orientation between the electric field of the incoming electromagnetic field and the molecule. Within the confocal volume, there must be orientation in the ensemble of individual crystallites. This effect is not visible when the measurement volume is large enough, compared to the different orientations, to cancel the effect of each other. These findings suggest that Raman imaging can be used to study molecular orientation at quite high resolution. They also indicate that intensity variations in Raman maps[72] may originate partially from orientation effects, in addition to concentration variations.

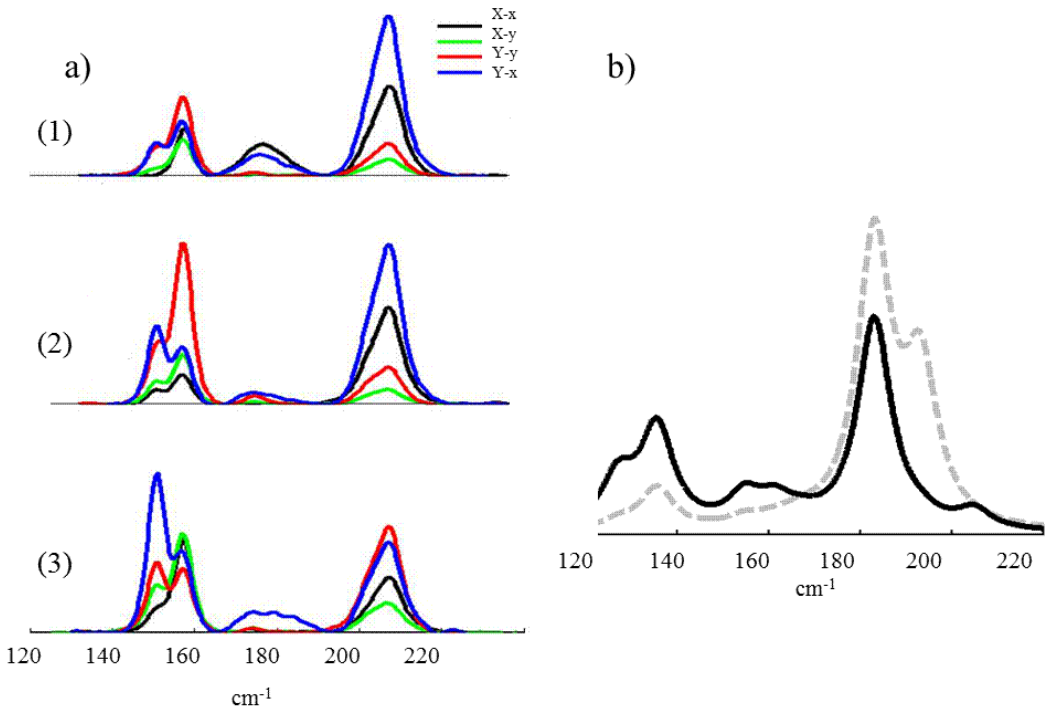

Figure 5.4 a) Laser and analyzer polarization dependent Raman spectrum measured from three different om-POSS particles. Upper-case letters define an analyzer polarization mode; lower-case letters are a laser polarization mode. Note that x and y means only that modes are orthogonal with respect to each other. Unpublished data. b) Calculated spectra with two different linearly polarized laser and analyzer (parallel) orientations: 60° (gray) and 180° (black) rotation around a trigonal axis of the rhombohedral om-POSS crystal. From Publication II. Copyright © 2011 NORD-IS

This material, 3 wt-% of om-POSS, had somewhat increased AC and DC breakdown strength; simultaneously, permittivity was slightly higher than reference PP.[72] This might be due to that om-POSS effects on the microstructure of PP or also that it might locally increase the thermal stability of PP under electric stress when high temperatures are present. It can act as a synergist in intumescence, a swelling of material, where a barrier is formed that acts as physical and thermal protection against a rapid increase of temperature by limiting heat and mass transfer between the gas and the condensed phase.[62] The amount of filler dispersed at nanoscale was very low in this composite despite all the effort to achieve good dispersion.

5.1.2 Crystalline filler: nano-$CaCO_3$

The PP with crystalline filler $CaCO_3$ was analyzed with coarse Raman imaging in addition to TEM analysis, and composites were found to contain well-dispersed nanoparticles and steadily increasing amounts of microparticles as the filler concentration was increased. (see Figure 5.5) There was no obvious correlation between NNI and skewness to DBS, but the parameters evaluating

the quality of dispersion were both under the limits previously suggested for optimal dielectric properties.[129] These numerical dispersion assessment methods are all relatively insensitive to volume fraction and primary particle size since they consider clusters as point objects. The evolution of these parameters with concentration is complex and no straight correlation can be expected. The maximum increase in DBS was achieved with 1.8 wt-% filler loading. The DBS decreased as the microparticles became more abundant, but the effect of the filler on increasing the permittivity of the material was subtle. (see Figure 5.6) Overall the addition of nano-$CaCO_3$ to PP did not much change the dielectric properties.

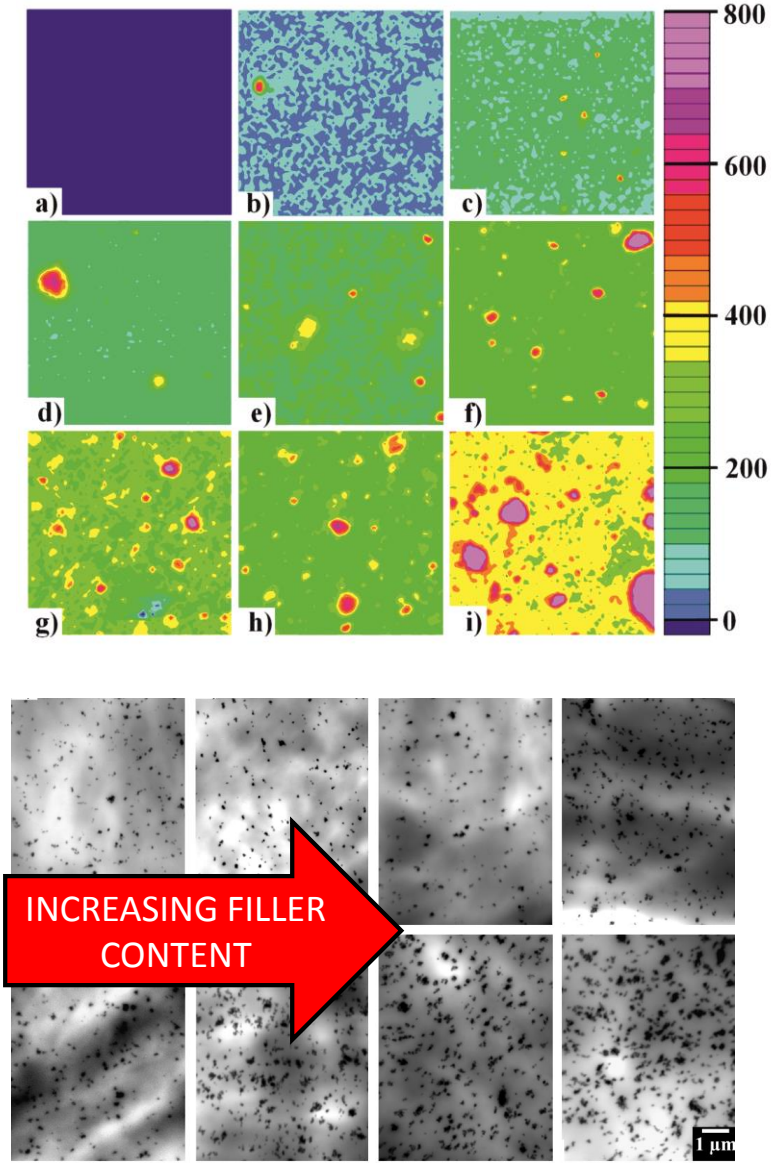

Figure 5.5 Raman contour maps (210 x 210 µm²) of cast samples, generated by integrating the most intense characteristic peak of $CaCO_3$: a) pure PP b) 1.8 wt-% c) 2.7 wt-% d) 3.6 wt-% e) 4.6 wt-% f) 5.6 wt-% g) 6.4 wt-% h) 7.4 wt-% and i) 8.1 wt-% nano-$CaCO_3$/PP composite sample. The overall level of the $CaCO_3$ signal rises as the concentration of nano-$CaCO_3$ increases in the composites. Shown below are TEM images from the same composites, showing gradually increasing concentration of the filler dispersed at nanoscale.

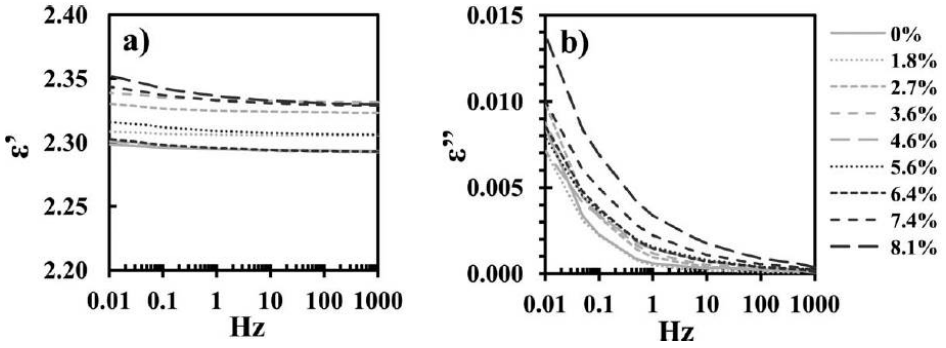

Figure 5.6 a) Real and b) imaginary parts of complex permittivity at different $CaCO_3$ contents in PP composites, as a function of frequency. This figure is from Publication III. Copyright© John Wiley and Sons, Inc.

5.1.3 Amorphous filler: fumed silica

Both AC and DC DBS of the composite increased substantially for 5 wt-% silica composite and the β-value, also known as the shape factor, is higher than with reference PP. The higher the value of β, the narrower the spread of individual results; this is an indication of a homogeneous material. Silica was found to disperse in PP as fractal agglomerates, around 100 nm in size. (see Figure 5.7) XPD and Raman studies found that this composite also contains $CaCO_3$, a contamination from an extruder. 3D-characterization of this composite by CμXT revealed $CaCO_3$ microcrystal loading to be 2.3 wt-% in this composite. But $CaCO_3$ alone is not responsible of the increased DBS,[III] so it must be effect caused by silica filler.

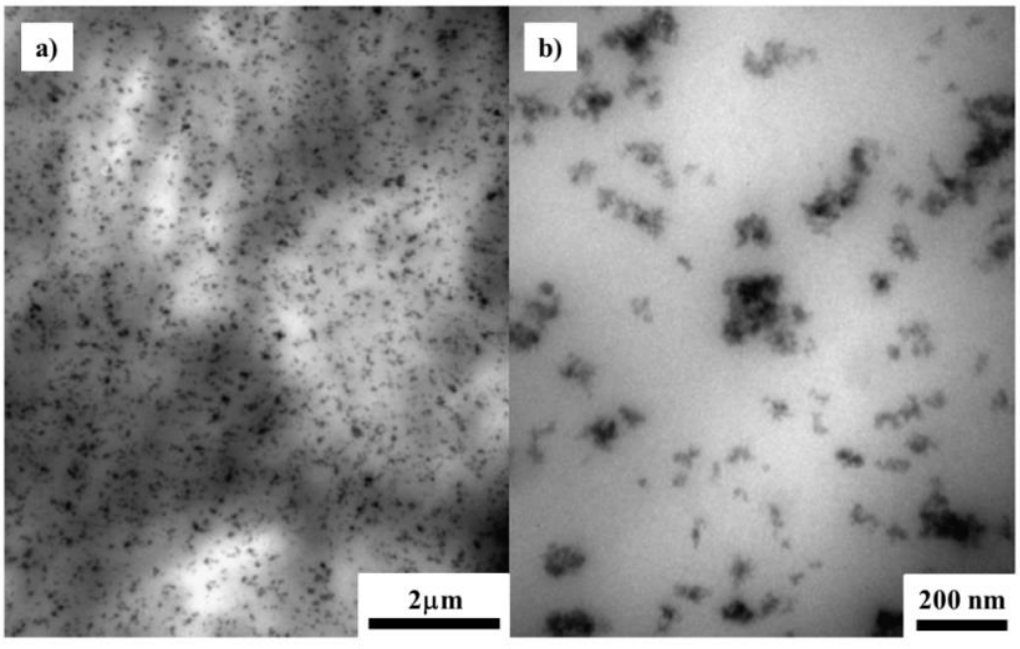

Figure 5.7 TEM images of 5 wt-% silica PP composite.

There was dramatic enhancement in partial discharge (PD) endurance of the composite compared to neat PP. Optical microscopy shows fractal structure formed in the composite due to PD stress; these might indicate that silica has some role in restricting the degradation of the composite as not as prominent structures were found in neat PP reference at any stress voltage used. (see Figure 5.8)

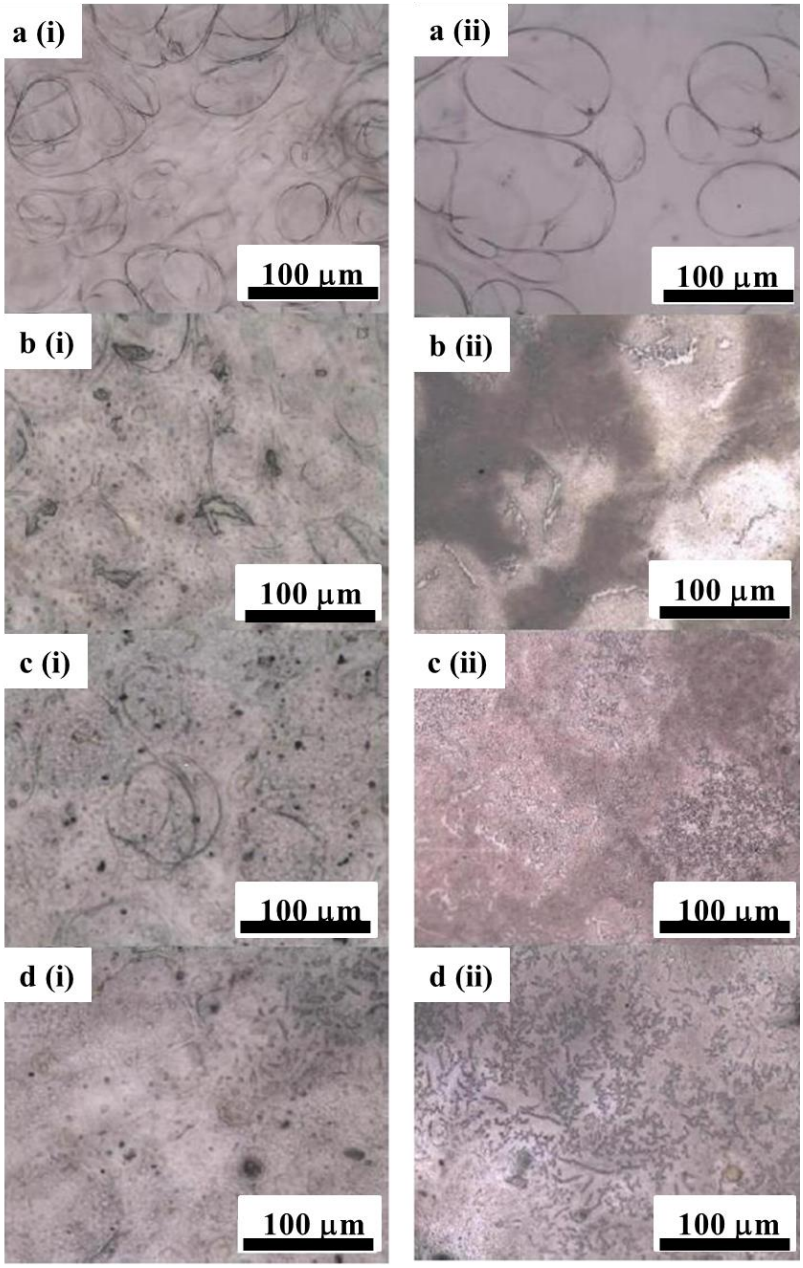

Figure 5.8 Optical microscope images of (i) PP and (ii) 5 wt-% silica PP composite: a) unstressed b) 2 kV c) 3 kV d) 4 kV stressed samples. See the fractal structures formed in composite under electrical stress.

5.2 Epoxy Composite

This section describes the results from Publication IV. The motivation was to get fundamental understanding of the role of the nanoparticle interface in controlling the material properties. It focuses on synthesis and dielectric properties of polymeric nanocomposites where silica nanoparticles are grafted with bimodal ligands: a short ligand; oligothiophene or ferrocene to control the electrical properties and a long epoxy compatible ligand (PGMA) that ensures optimal dispersion.

5.2.1 Colloidal filler: bimodal-polymer-brush-grafted silica

A new synthetic approach was used to provide well-dispersed silica particles with electroactive core functionalization in epoxy in order to study the effect of the charge layer at the interface of the nanoparticle and polymer matrix. (see Figure 5.9) Dispersion of the filler using this approach is so effective that most of the materials are optically transparent, (see Figure 5.10) especially composites with bimodal silica with thiophene as its functionality, had outstanding dispersion and electrical properties. Significant increases in the DBS were represented by the 63.2-% (α) parameter from the Weibull distribution plus the threshold parameter. 2 wt-% silica grafted with PGMA and oligothiophene and 4 wt-% silica grafted with PGMA and ferrocene provided an increase in the 63.2% average DBS α of greater than 40%. The free-space length, L_f, and DBS α 63.2% average with shape factor are shown in Table 5.1. The increase in DBS is well correlated to a decrease in L_f. For example, a comparison between the bare silica and the PGMA modified silica shows a significant improvement in DBS corresponding to a large decrease in L_f. It seems that distribution of electroactive nanofiller must be dense enough to give the greatest improvement in DBS. If dense enough distribution of particles was achieved, then the DBS increased considerably. (see Figure 5.11 and table 5.1)

It is obvious that the electroactivity at the silica particle core is largely responsible for the improvements to the DBS. Even if similar good dispersion is achieved with PGMA modified silica filler, the small improvement in DBS indicates that the silica filler itself is not alone responsible for the improvements seen in the modified filler composites. Another indication is that even if the particle dispersion is not optimal, as in silica-PGMA-ferrocene composites, improvement is still seen in DBS.

Promising for future applications is that permittivity increased 25% with only 2 wt-% filler loading as dielectric loss stayed at the level of reference epoxy. If there were also microaggregates in the material, as in 4 wt-% silica-PGMA-ferrocene, low frequency losses increased. (see Figure 5.12)

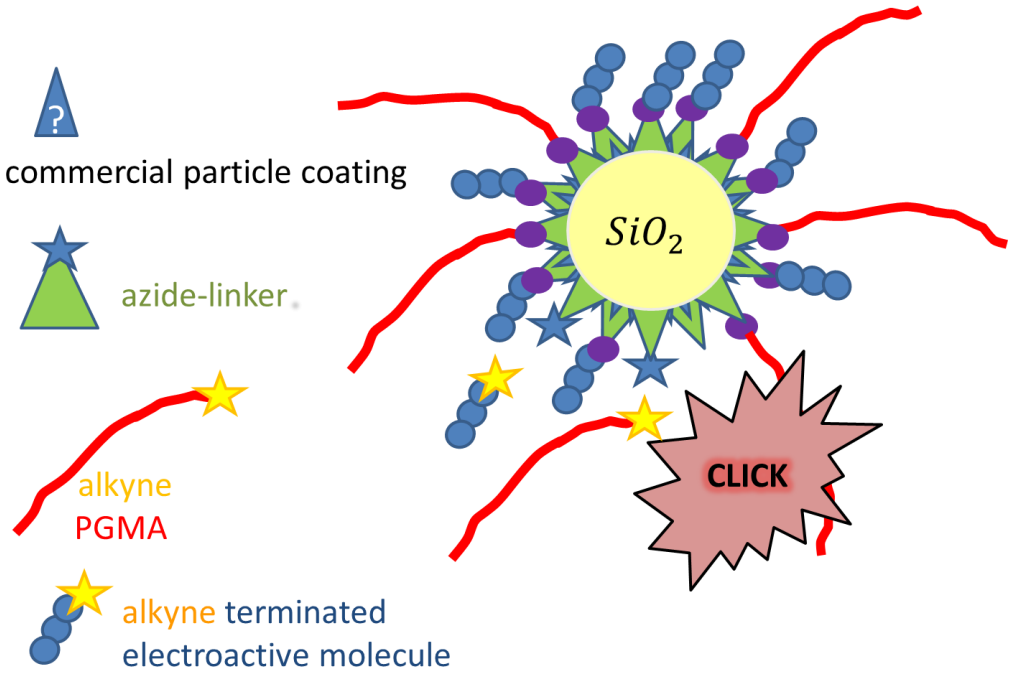

Figure 5.9 Schematic model of bimodal polymer grafted core functionalized colloidal silica particle.

Figure 5.10 Visual transparencies of some epoxy composite blocks with different silica contents/surface modifications. From left: 1 wt-% bare silica, 2 wt-% silica-PGMA, 2 wt-% silica-PGMA-oligothiophene and 4 wt-% silica-PGMA-ferrocene in epoxy.

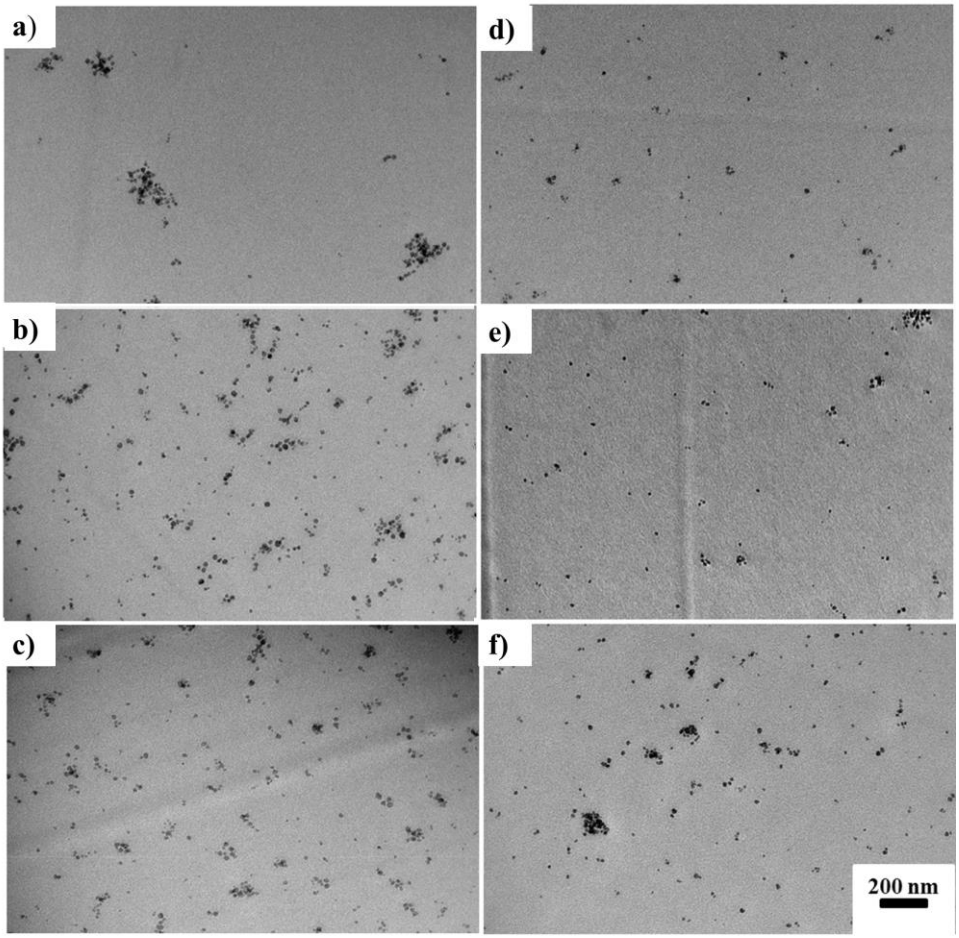

Figure 5.11 TEM images of epoxy composites with: a) 1 wt-% bare silica b) 2 wt-% silica-PGMA c) 2 wt-% silica-PGMA-oligothiophene d) 1 wt-% silica-PGMA-ferrocene e) 2 wt-% silica-PGMA-ferrocene f) 4 wt-% silica-PGMA-ferrocene

Table 5.1 The free-space length (L_f) between filler particles and 63.2-%(α) DBS and shape factor (β) from measured samples.

Sample	L_f (nm)	DBS	
		α (kV/mm)	β
neat epoxy	NA	185	1.4
1 wt-% bare SiO_2	900	182	1.6
2 wt-% SiO_2-PGMA	250	213	1.4
1 wt-% SiO_2-PGMA-ferro	600	236	1.5
2 wt-% SiO_2-PGMA-ferro	550	235	1.4
4 wt-% SiO_2-PGMA-ferro	300	265	1.8
2 wt-% SiO_2-PGMA-thio	250	266	1.9

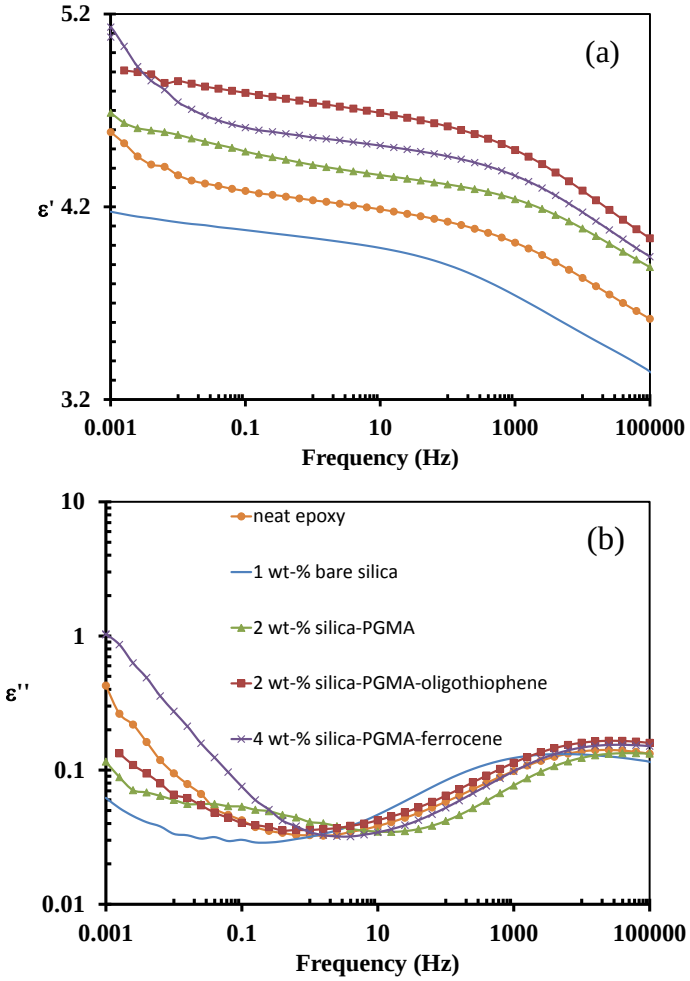

Figure 5.12 a) Dielectric permittivity b) Dielectric losses as a function of frequency for neat epoxy, bare silica filled composite and for composites that have an electroactive layer and epoxy compatible polymer layer on the core of the filler particle core.

6 SUMMARY AND CONCLUSIONS

Studies of multiscale structure and dielectric properties of PP doped with om-POSS, nano-$CaCO_3$ and fumed silica were carried out. All these composites showed improvement in their dielectric properties, especially DBS was increased. In all of these composites only part of the filler was found to be dispersed at nanoscale. When composite material consisting of a molecular filler om-POSS and PP was studied by confocal Raman micro-spectroscopy, it was found that the relative intensities of different Raman peaks of om-POSS varied depending on the measurement spot. Multiscale characterization yielded a detailed picture of the samples consisting of homogeneously distributed micron-sized elongated om-POSS agglomerates. The variation in the Raman spectra of these can be explained by the orientation of crystallites, showing that, within the confocal volume, there is orientation in the ensemble of crystallites forming large agglomerates. The results are important considering the interpretation of Raman images in composite materials and imply a possibility for orientational imaging. The structure of the composite with crystalline filler $CaCO_3$ was determined using TEM and coarse Raman imaging; which allow screening of larger areas from a sample. Dielectric measurements indicate that DC breakdown strength increases slightly with 1.8 wt-% of $CaCO_3$, but then decreases as a function of concentration, largely owing to an increase of low-field breakdowns likely caused by the large microparticles present in the material. Thus, the positive effect of nanodispersion is masked by the negative effect caused by microparticles. Raman microscopy is shown to be a particularly informative technique to reveal structural information at the nano- and microscale. The amorphous silica composite showed improved the DBS and especially high PD endurance. Silica was dispersed as fractal agglomerates in the composite. All the results demonstrate the importance of multiscale structural analysis of composite samples when studying the effect of structure on dielectric properties.

A new synthetic approach was used to afford well-dispersed silica particles with electroactive core functionalization in epoxy in order to be able to study the effects of the charge layer at the interface of the nanoparticle and polymer matrix. The long, epoxy compatible PGMA brush ensured good disper-

sion and allowed study of the effect of the electroactive layer on the breakdown strength. The DBS and permittivity increased considerably in the bimodal brush particle composites. Still more studies are needed to get more detailed picture of why the electroactive layer at the nanoparticle core improves dielectric breakdown strength of the polymer composite. However, this can only be done if the dispersion of particles in the composite at the nanoscale is possible. Bimodal ligand engineering seems to be a good approach to achieve that.

REFERENCES

1. R. Hackam, Outdoor high voltage polymeric insulators, *Electrical Insulating Materials,. Proceedings of 1998 International Symposium on,* **1998**, 1-16.

2. S. Kumagai and N. Yoshimura, Leakage Current Characterization for Estimating the Conditions of Ceramic and Polymeric Insulating Surfaces, *IEEE Trans. Dielectr. Electr. Insul.* **2004**, *11,* 681-690.

3. Q. Wang and L. Zhu, Polymer Nanocomposites for Electrical Energy Storage, *J. Polym. Sci. Pt. B-Polym. Phys.* **2011**, *49,* 1421-1429.

4. C. Mayoux, Studies on the Aging Processes of Polymers in Electrical Systems, *Angew. Makromol. Chem.* **1998**, *262,* 143-156.

5. T. J. Lewis, Ageing - A Perspective, *IEEE Electr. Insul. Mag.* **2001**, *17,* 6-16.

6. C. A. Spellman, H. M. Young, A. Haddad, A. R. Rowlands and R. T. Waters, Survey of Polymeric Insulator Ageing Factors, *High Voltage Engineering, 1999. 11th International Symposium on (Conf. Publ. No. 467),* **1999,** *4,* 160-163.

7. C. Laurent and G. Teyssedre, Hot Electron and Partial-discharge Induced Ageing of Polymers, *Nucl. Instrum. Meth. B.* **2003**, *208,* 442-447.

8. J. P. Crine, On the Interpretation of Some Electrical Aging and Relaxation Phenomena in Solid Dielectrics, *IEEE Trans. Dielectr. Electr. Insul.* **2005**, *12,* 1089-1107.

9. T. Tanaka, Dielectric Nanocomposites with Insulating Properties, *IEEE Trans. Dielectr. Electr. Insul.* **2005**, *12,* 914-928.

10. M. F. Frechette, M. L. Trudeau, H. D. Alamdari and S. Boily, Introductory Remarks on Nanodielectrics, *IEEE Trans. Dielectr. Electr. Insul.* **2004**, *11,* 808-818.

11. W. C. Johnson, Electronic Transport in Insulating Films, *IEEE Trans. Nucl. Sci.* **1972**, *19,* 33.

12. J. Lewiner, Evolution of Experimental Techniques for The Study of The Electrical Properties of Insulating Materials, *IEEE Trans. Dielectr. Electr. Insul.* **1986**, *EI-21 No.3*.

13. J. E. Murphy and S. O. Morgan, Dielectric Properties of Insulating Materials, *Bell Systems Technical Journal.* **1937**, *16,* 493.

14. H. M. Rosenberg, *The solid state,* 2nd edition, Clarendon Press, California, **1978**.

15. A. K. Jonscher, Dielectric Relaxation in Solids, *J. Phys. D: Appl. Phys.* **1999**, *32,* R57.

16. G. G. Raju, *Dielectrics in Electric Fields,* 1st edition, Marcel Dekker, New York, **2003**.

17. C. Le Gressus and G. Blaise, Breakdown Phenomena Related To Trapping/Detrapping Processes In Wide Band Gap Insulators, *IEEE Trans. Dielectr. Electr. Insul.* **1992**, *32 No3,* 472.

18. M. Meunier, N. Quirke and A. Aslanides, Molecular Modeling of Electron Traps in Polymer Insulators: Chemical Defects and Impurities, *J. Chem. Phys.* **2001**, *115,* 2876-2881.

19. C. Zener, A Theory of the Electrical Breakdown of Solid Dielectrics, *Proceedings of the Royal Society of London. Series A*. **1934**, *145,* 523-529.

20. J. J. Odwyer, Theory of Avalanche Breakdown in Solid Dielectrics, *Journal of Physics and Chemistry of Solids.* **1967**, *28,* 1137.

21. J. J. Odwyer, Theory of Dielectric Breakdown in Solids, *J. Electrochem. Soc.* **1969**, *116,* 239.

22. M. Ieda, Dielectric-Breakdown Process of Polymers, *IEEETrans. Dielectr. Electr. Insul*. **1980**, *15,* 206-224.

23. N. Shimizu and C. Laurent, Electrical Tree Initiation, *IEEE Trans. Dielectr. Electr. Insul.* **1998**, *5,* 651-659.

24. T. Tanaka, G. C. Montanari and R. Mulhaupt, Polymer Nanocomposites as Dielectrics and Electrical Insulation-Perspectives for Processing Technologies, Mate-

rial Characterization and Future Applications, *IEEE Trans. Dielectr. Electr. Insul.* **2004**, *11,* 763-784.

25. T. J. Lewis, Nanometric Dielectrics, *IEEE Trans. Dielectr. Electr. Insul.* **1994**, *1,* 812-825.

26. J. Keith Nelson, *Dielectric Polymer Nanocomposites.* In book: J. K. Nelson (edit.), *Background, Principles and Promise of Nanodielectrics,* Springer, New York, **2010**, 368.

27. M. G. Danikas and T. Tanaka, Nanocomposites-A Review of Electrical Treeing and Breakdown, *IEEE Electr. Insul. Mag.* **2009**, *25,* 19-25.

28. N. Silvi, M. Giammattei, P. C. Irwin, Y. Cao, Q.T. Daniel and C. Mead, Biaxially Oriented Nanocomposite Film, Method of Manufacture, and Articles Thereof, *Biaxially Oriented Nanocomposite Film, Method of Manufacture, and Articles Thereof,* US 20090226711 A1, 10 Sep **2009.**

29. T. P. Schuman, S. Siddabattuni, O. Cox and F. Dogan, Improved Dielectric Breakdown Strength of Covalently-Bonded Interface Polymer-Particle Nanocomposites, *Composite Interfaces.* **2010**, *17,* 719-731.

30. H. Tang and H. A. Sodano, High energy density nanocomposite capacitors using non-ferroelectric nanowires, *Appl. Phys. Lett.* **2013**, *102,* 063901.

31. L. A. Fredin, Z. Li, M. T. Lanagan, M. A. Ratner and T. J. Marks, Sustainable High Capacitance at High Frequencies: Metallic Aluminum - Polypropylene Nanocomposites, *ACS Nano.* **2013**, *7,* 396-407.

32. D. Pitsa, G. Vardakis, M. G. Danikas and M. Kozako, Electrical Treeing Propagation in Nanocomposites and the Role of Nanofillers: Simulation with the Aid of Cellular Automata, *Journal of Electrical Engineering-Elektrotechnicky Casopis.* **2010**, *61,* 125-128.

33. T. J. Lewis, Interfaces are the Dominant Feature of Dielectrics at the Nanometric Level, *IEEE Trans. Dielectr. Electr. Insul.* **2004**, *11,* 739-753.

34. G. Gouy, *Comt. Rend.* **1909**, *149,* 654.

35. D. L. Chapman, *Phil. Mag.* **1913**, *(6)25,* 475.

36. G. Tsagaropoulos and A. Eisenberg, Dynamic-Mechanical Study of the Factors Affecting theTwo Glass-Transition Behavior of Filled Polymers - Similarities and Differences with Random Ionomers, *Macromolecules.* **1995**, *28,* 6067-6077.

37. C. A. Grabowski, S. P. Fillery, N. M. Westing, C. Chi, J. S. Meth, M. F. Durstock and R. A. Vaia, Dielectric Breakdown in Silica-Amorphous Polymer Nanocom-

posite Films: The Role of the Polymer Matrix, *ACS Appl. Mater. Interfaces.* **2013**, *5,* 5486-5492.

38. S. Siddabattuni, T. P. Schuman and F. Dogan, Dielectric Properties of Polymer-Particle Nanocomposites Influenced by Electronic Nature of Filler Surfaces, *ACS Appl. Mater. Interfaces.* **2013**, *5,* 1917-1927.

39. C. Green and A. Vaughan, Nanodielectrics - How Much Do We Really Understand?, *Electrical Insulation Magazine, IEEE.* **2008**, *24,* 6-16.

40. Y. Cao, P. C. Irwin and K. Younsi, The Future of Nanodielectrics in the Electrical Power Industry, *IEEE Trans. Dielectr. Electr. Insul.* **2004**, *11,* 797-807.

41. A. S. Vaughan, Y. Zhao, L. L. Barre, S. J. Sutton and S. G. Swingler, On additives, Morphological Evolution and Dielectric Breakdown in Low Density Polyethylene, *Eur. Polym. J.* **2003**, *39,* 355-365.

42. J. K: Nelson, Y. Hu and J. Thiticharoenpong, Electrical Properties of $Ti0_2$ Nanocomposites, *2003 Annual Report Conference on Electrical Insulation and Dielectric Phenomena,* **2003**, 719-722.

43. A. C. Balazs, T. Emrick and T. P. Russell, Nanoparticle Polymer Composites: Where Two Small Worlds Meet, *Science.* **2006**, *314,* 1107-1110.

44. J. Jancar, J. F. Douglas, F. W. Starr, S. K. Kumar, P. Cassagnau, A. J. Lesser, S. S. Sternstein and M. J. Buehler, Current Issues in Research on Structure-Property Relationships in Polymer Nanocomposites, *Polymer.* **2010**, *51,* 3321-3343.

45. A. Okada and A. Usuki, Twenty Years of Polymer-Clay Nanocomposites, *Macromol. Mater. Eng.* **2006**, *291,* 1449-1476.

46. D. R. Paul and L. M. Robeson, Polymer nanotechnology: Nanocomposites, *Polymer.* **2008**, *49,* 3187-3204.

47. M. Z. Rong, M. Q. Zhang and W. H. Ruan, Surface Modification of Nanoscale Fillers for Improving Properties of Polymer Nanocomposites: a Review, *Mater. Sci. Technol.* **2006**, *22,* 787-796.

48. D. W. Schaefer and R. S. Justice, How nano are nanocomposites? *Macromolecules.* **2007**, *40,* 8501-8517.

49. S. C. Tjong, Structural and Mechanical Properties of Polymer Nanocomposites, *Mater. Sci. Eng.:R.* **2006**, *53,* 73-197.

50. C. L. Wu, M. Q. Zhang, M. Z. Rong and K. Friedrich, Tensile Performance Improvement of Low Nanoparticles Filled-polypropylene Composites, *Composites Sci. Technol.* **2002**, *62,* 1327-1340.

51. V. Busico and R. Cipullo, Microstructure of Polypropylene, *Prog. Polym. Sci.* **2001**, *26,* 443-533.

52. H. D. Keith, F. J. Padden, N. M. Walter and H. W. Wyckoff, Evidence for a Second Crystal Form of Polypropylene, *J. Appl. Phys.* **1959**, *30,* 1485-1488.

53. F. J. Padden and H. D. Keith, Spherulitic Crystallization in Polypropylene, *J. Appl. Phys.* **1959**, *30,* 1479-1484.

54. F. A. Bovey, *Macromolecules: An Introduction to Polymer Science,* 1st edition, Academic Press, **1979**, 328.

55. J. Karger-Kocsis, *Polypropylene 1. Copolymers and blends.* In book: J. Peterman (edit.), *Epitaxial growth in and with polypropylene,* Chapman & Hall, London, UK, **1995**, 351.

56. International Centre for Diffraction Data, *ICDD-PDF2,* Release 2007, Pennsylvania, USA, **2007**.

57. Y. Cong, Z. Hong, W. Zhou, W. Chen, F. Su, H. Li, X. Li, K. Yang, X. Yu, Z. Qi and L. Li, Conformational Ordering on the Growth Front of Isotactic Polypropylene Spherulite, *Macromolecules.* **2012**, *45,* 8674-8680.

58. D. Kim, J. S. Lee, C. F. Barry and J. L. Mead, Evaluation and Prediction of The Effects of Melt-Processing Conditions on the Degree of Mixing in Alumina/Poly(Ethylene Terephthalate) Nanocomposites, *J. Appl. Polym. Sci.* **2008**, *109,* 2924-2934.

59. K. S. V. Srinivasan, Macromolecules: New Frontiers: Proceedings of the IUPAC International Symposium on Advances in Polymer Science and Technology, MACRO-98, January 5-9, **1998**.

60. S. J. Laihonen, Polypropylene: Morphology, Defects and Electrical Breakdown, KTH, **2005**.

61. S. H. Phillips, T. S. Haddad and S. J. Tomczak, Developments in Nanoscience: Polyhedral Oligomeric Silsesquioxane (POSS)-Polymers, *Current Opinion in Solid State and Materials Science.* **2004**, *8,* 21-29.

62. A. Vannier, S. Duquesne, S. Bourbigot, A. Castrovinci, G. Camino and R. Delobel, The Use of POSS as Synergist in Intumescent Recycled Poly(ethylene terephthalate). *Polym. Degrad. Stab.* **2008**, *93,* 818-826.

63. J. Wu and P. T. Mather, POSS Polymers: Physical Properties and Biomaterials Applications, *Polymer Reviews.* **2009**, *49,* 25-63.

64. S. -W Kuo and F. -C Chang, POSS Related Polymer Nanocomposites, *Prog. Polym. Sci.* **2011**, *36,* 1649-1696.

65. E. Ayandele, B. Sarkar and P. Alexandridis, Polyhedral Oligomeric Silsesquioxane (POSS)-Containing Polymer Nanocomposites, *Nanomaterials.* **2012**, *2,* 445-475.

66. B. X. Fu, M. Y. Gelfer, B. S. Hsiao, S. Phillips, B. Viers, R. Blanski and P. Ruth, Physical Gelation in Ethylene–Propylene Copolymer Melts Induced by Polyhedral Oligomeric Silsesquioxane (POSS) Molecules, *Polymer.* **2003**, *44,* 1499-1506.

67. M. Pracella, D. Chionna, A. Fina, D. Tabuani, A. Frache and G. i. Camino, Polypropylene-POSS Nanocomposites: Morphology and Crystallization Behaviour. *Macromol. Symp.* **2006**, *234,* 59-67.

68. F. Baldi, F. Bignotti, A. Fina, D. Tabuani and T. Ricco, Mechanical Characterization of Polyhedral Oligomeric Silsesquioxane/Polypropylene Blends. *J. Appl. Polym. Sci.* **2007**, *105,* 935-943.

69. A. Fina, D. Tabuani, A. Frache and G. Camino, Polypropylene-Polyhedral Oligomeric Silsesquioxanes (POSS) Nanocomposites. *Polymer.* **2005**, *46,* 7855-7866.

70. C. Y. Jung, H. S. Kim, H. J. Hah and S. M. Koo, Self-assembly Growth Process for Polyhedral Oligomeric Silsesquioxane Cubic Crystals. *Chem. Commun. (Cambridge, U. K.).* **2009,** *10,* 1219-1221.

71. M. Joshi and B. S. Butola, Isothermal Crystallization of HDPE/Octamethyl Polyhedral Oligomeric Silsesquioxane Nanocomposites: Role of POSS as a Nanofiller. *J. Appl. Polym. Sci.* **2007**, *105,* 978-985.

72. M. Takala, M. Karttunen, P. Salovaara, S. Kortet, K. Kannus and T. Kalliohaka, Dielectric Properties of Nanostructured Polypropylene- Polyhedral Oligomeric Silsesquioxane Compounds. *IEEE Trans. Dielectr. Electr. Insul.* **2008**, *15,* 40-51.

73. J. Horwath, D. Schweickart, G. Garcia, D. Klosterman and M. Galaska, Improved performance of Polyhedral Oligomeric Silsesquioxane Epoxies, *Electrical Insulation and Dielectric Phenomena, 2005. CEIDP '05. 2005 Annual Report Conference on,* ss. 155-157.

74. K. Gorna, M. Hund, M. Vucak, F. Groehn and G. Wegner, Amorphous Calcium Carbonate in Form of Spherical Nanosized Particles and Its Application as Fillers for Polymers, *Mater. Sci. Eng.: A.* **2008**, *477,* 217-225.

75. W. C. J. Zuiderduin, C. Westzaan, J. Huetink and R. J. Gaymans, Toughening of Polypropylene with Calcium Carbonate Particles, *Polymer.* **2003**, *44,* 261-275.

76. J. I. Weon, K. T. Gam, W. J. Boo, H.J Sue and C. M. Chan, Impact-toughening Mechanisms of Calcium Carbonate-reinforced Polypropylene Nanocomposite, *J. Appl. Polym. Sci.* **2006**, *99,* 3070-3076.

77. M. -R Meng and Q. Dou, Effect of Filler Treatment on Crystallization, Morphology and Mechanical Properties of Polypropylene/Calcium Carbonate Composites, *J. Macromol. Sci. B: Phys.* **2009**, *48,* 213-225.

78. M. Y. A. Fuad, H. Hanim, R. Zarina, Z. A. M. Ishak and A. Hassan, Polypropylene/Calcium Carbonate Nanocomposites - Effects of Processing Techniques and Maleated Polypropylene Compatibiliser, *Express Polymer Letters.* **2010**, *4,* 611-620.

79. H. Huang, B. Han, L. Wang, N. Miao, H. Mo, N. -L Zhou, Z. -M Ma, J. Zhang and J. Shen, Crystallization Kinetics of Polypropylene Composites Filled with Nano Calcium Carbonate Modified with Maleic Anhydride, *J. Appl. Polym. Sci.* **2011**, *119,* 1516-1527.

80. Y. S. Thio, A. S. Argon, R. E. Cohen and M. Weinberg, Toughening of Isotactic Polypropylene with $CaCO_3$ Particles, *Polymer.* **2002**, *43,* 3661-3674.

81. D. Eiras and L. A. Pessan, Mechanical Properties of Polypropylene/Calcium Carbonate Nanocomposites, *Mat. Res.* **2009**, *12,* 517-522.

82. M. Q. Zhang, M. Z. Rong, S. L. Pan and K. Friedrich, Tensile Properties of Polypropylene Filled with Nanoscale Calcium Carbonate Particles, *Adv. Compos. Lett.* **2002**, *11,* 293-298.

83. Y. Wang and W. C. Lee, Interfacial Interactions in Calcium Carbonate-Polypropylene Composites. 1: Surface Characterization and Treatment of Calcium Carbonate: A Comparative Study, *Polymer Composites.* **2003**, *24,* 119-131.

84. Q. X. Zhang, Z. Z. Yu, X. L. Xie and Y. W. Mai, Crystallization and Impact Energy of Polypropylene/$CaCO_3$ Nanocomposites with Nonionic Modifier, *Polymer.* **2004**, *45,* 5985-5994.

85. Y. Wang and W. C. Lee, Interfacial Interactions in Calcium Carbonate-Polypropylene Composites. 2: Effect of Compounding on the Dispersion and the Impact Properties of Surface-Modified Composites, *Polymer Composites.* **2004**, *25,* 451-460.

86. Z. Lin, Z. Z. Huang, Y. Zhang, K. C. Mai and H. M. Zeng, Crystallization and Melting Behavior of Nano-$CaCO_3$/Polypropylene Composites Modified by Acrylic Acid, *J. Appl. Polym. Sci.* **2004**, *91,* 2443-2453.

87. W. Wan, D. Yu, Y. Xie, X. Guo, W. Zhou and J. Cao, Effects of Nanoparticle Treatment on the Crystallization Behavior and Mechanical Properties of Poly-

propylene/Calcium Carbonate Nanocomposites, *J. Appl. Polym. Sci.* **2006**, *102,* 3480-3488.

88. M. Avella, S. Cosco, M. L. Di Lorenzo, E. Di Pace, M. E. Errico and G. Gentile, Nucleation Activity of Nanosized $CaCO_3$ on Crystallization of Isotactic Polypropylene, in Dependence on Crystal Modification, Particle Shape, and Coating, *Eur. Polym. J.* **2006**, *42,* 1548-1557.

89. B. Cioni and A. Lazzeri, The Role of Interfacial Interactions in the Toughening of Precipitated Calcium Carbonate-Polypropylene Nanocomposites, *Composite Interfaces.* **2010**, *17,* 533-549.

90. P. Eteläaho, S. Haveri and P. Järvelä, Comparison of the Morphology and Mechanical Properties of Unmodified and Surface-Modified Nanosized Calcium Carbonate in a Polypropylene Matrix, *Polymer Composites.* **2011**, *32,* 464-471.

91. Y. Lin, H. Chen, C. -M Chan and J. Wu, Effects of Coating Amount and Particle Concentration on the Impact Toughness of Polypropylene/$CaCO_3$ Nanocomposites, *Eur. Pol. J.* **2011**, *47,* 294-304.

92. M. Kamal, C. S. Sharma, P. Upadhyaya, V. Verma, K. N. Pandey, V. Kumar and D. D. Agrawal, Calcium Carbonate ($CaCO_3$) Nanoparticle Filled Polypropylene: Effect of Particle Surface Treatment on Mechanical, Thermal, and Morphological Performance of Composites, *J. Appl. Polym. Sci.* **2012**, *124,* 2649-2656.

93. D. Garcia-Lopez, J. C. Merino and J. M. Pastor, Influence of the $CaCO_3$ Nanoparticles on the Molecular Orientation of the Polypropylene Matrix, *J. Appl. Polym. Sci.* **2003**, *88,* 947-952.

94. A. Qaiss, H. Saidi, O. Fassi-Fehri and M. Bousmina, Porosity Formation by Biaxial Stretching in Polyolefin Films Filled with Calcium Carbonate Particles, *J Appl. Polym. Sci.* **2012**, *123,* 3425-3436.

95. J. Zhang, H. Xie and X. Liu, Morphology and Electrical Breakdown of Polypropylene Morphology and Electrical Breakdown of Polypropylene, *International Conference on Properties and Applications of Dielectric Materials,* **1991**, *3*,1161.

96. K. Nevalainen, S. Auvinen, O. Orell, P. Eteläaho, R. Suihkonen, J. Vuorinen and P. Järvelä, Characterization of Melt-Compounded and Masterbatch-Diluted Polypropylene Composites Filled with Several Fillers, *J. Appl. Polym. Sci.* **2013**, *34,* 554-569.

97. M. H. Vakili, H. Ebadi-Dehaghani and M. Haghshenas-Fard, Crystallization and Thermal Conductivity of $CaCO_3$ Nanoparticle Filled Polypropylene, *J. Macrom. Sci. B: Phys.* **2011**, *50,* 1637-1645.

98. G. Bangehyi, G. Marosi, G. Bertalan and F. E. Karasz, Studies of Thermally Stimulated Current in Polypropylene Calcium-Carbonate Surfactant Systems, *Colloid Polym. Sci.* **1992**, *270,* 113-127.

99. W. Wan, D. Yu, Y. Xie, X. Guo, Z. Mao and L. Huang, Effects of Nanoparticle Surface Treatment on the Crystalline Morphology and Dielectric Property of Polypropylene/Calcium Carbonate Nanocomposites, *1st IEEE International Conference on Nano/Micro Engineered and Molecular Systems.* **2006**.

100. M. Takala, S. Kortet, P. Salovaara, M. Karttunen and K. Kannus, AC Breakdown Strenght of Polypropylene-Calcium Carbonate Compounds, *NORD-IS07.* **2007**.

101. C. T. Dervos, J. A. Mergos and A. A. Iosifides, Characterization of Insulating Particles by Dielectric Spectroscopy: Case Study for $CaCO_3$ Powders, *Mater Lett.* **2005**, *59,* 2842-2849.

102. H. E. Bergna and W. O. Roberts, *Colloidal Silica: Fundamentals and Applications,* CRC Press, **2005**.

103. J. P. Vigoroux, J. P. Duraud, A. Lemoel, C. LeGressus and D. L. Griscom, Electron Trapping in Amorphous SiO_2 Studied by Charge Buildup Under Electron-Bombardment, *J. Appl. Phys.* **1985**, *57,* 5139-5144.

104. A.K. Schlarb, D.N. Suwitaningsih, M. Kopnarski and G. Niedner-Schatteburg, Supermolecular Morphology of Polypropylene Filled with Nanosized Silica, *J. Appl. Polym. Sci.* **2013** DOI: 10.1002/app.39655

105. S. Zhang, A. Zhu and S. Dai, Coincorporation of Nano-Silica and Nano-Calcium Carbonate in Polypropylene, *J. Appl. Polym. Sci.* **2011**, *121,* 3007-3013.

106. P. O. Henk, T. W. Kortsen and T. Kvarts, Increasing the Electrical Discharge Endurance of Acid Anhydride Cured DGEBA Epoxy Resin by Dispersion of Nanoparticle Silica, *High Perform. Polymers.* **1999**, *11,* 281-296.

107. M. Roy, J. K. Nelson, R. K. MacCrone, L. S. Schadler, C. W. Reed, R. Keefe and W. Zenger, Polymer Nanocomposite Dielectrics - The role of the Interface, *IEEE Trans. Dielectr. Electr. Insul.* **2005**, *12,* 629-643.

108. M. Roy, J. Nelson, R. K. MacCrone and L. S. Schadler, Candidate Mechanisms Controlling the Electrical Characteristics of Silica/XLPE Nanodielectrics, *J. Mater. Sci.* **2007**, *42,* 3789-3799.

109. J. D. Lemay and F. N. Kelley, Structure and Ultimate Properties of Epoxy-Resins, *Adv. Pol. Sci.* **1986**, *78,* 115-148.

110. C. Augustsson, *NM Epoxy Handbook,* 3rd edition, Nils Malmgren AB, Sweden, **2004**.

111. B. –L. Denq, Y. –S. Hu, L. –W. Chen, W. –Y. Chiu and T. –R. Wu, The Curing Reaction and Physical Properties of DGEBA/DETA Epoxy Resin Blended with Propyl Ester Phosphazene, *J. Appl. Polym. Sci.* **1999**, *74,* 229-237.

112. H. Gao and K. Matyjaszewski, Synthesis of Molecular Brushes by "Grafting onto" method: Combination of ATRP and Click Reactions, *J. Am. Chem. Soc.* **2007**, *129,* 6633-6639.

113. G. D. Smith and D. Bedrov, Dispersing Nanoparticles in a Polymer Matrix: Are Long, Dense Polymer Tethers Really Necessary? *Langmuir.* **2009**, *25,* 11239-11243.

114. Y. Li, P. Tao, A. Viswanath, B. C. Benicewicz and L. S. Schadler, Bimodal Surface Ligand Engineering: The Key to Tunable Nanocomposites, *Langmuir.* **2013**, *29,* 1211-1220.

115. V. D. Bock, H. Hiemstra and J. H. van Maarseveen, Cu-I-catalyzed Alkyne-Azide "Click" Cycloadditions from a Mechanistic and Synthetic Perspective, *Eur. J. Org. Chem.* **2006,** *1,* 51-68.

116. J. E. Moses and A. D. Moorhouse, The Growing Applications of Click Chemistry, *Chem. Soc. Rev.* **2007**, *36,* 1249-1262.

117. H. C. Kolb, M. G. Finn and K. B. Sharpless, Click Chemistry: Diverse Chemical Function from a Few Good Reactions, *Angew. Chem. Int. Ed.* **2001**, *40,* 2004-+.

118. T. Lummerstorfer and H. Hoffmann, Click Chemistry on Surfaces: 1,3-dipolar Cycloaddition Reactions of Azide-terminated Monolayers on Silica, *J. Phys. Chem B.* **2004**, *108,* 3963-3966.

119. Y. Wang, J. Chen, J. Xiang, H. Li, Y. Shen, X. Gao and Y. Liang, Synthesis and Characterization of End-functional Polymers on Silica Nanoparticles via a Combination of Atom Transfer Radical Polymerization and Click Chemistry, *React. Funct. Polym.* **2009**, *69,* 393-399.

120. R. Ranjan and W. J. Brittain, Tandem RAFT Polymerization and Click Chemistry: An Efficient Approach to Surface Modification, *Macromol. Rapid Commun.* **2007**, *28,* 2084-2089.

121. R. Ranjan and W. J. Brittain, Combination of Living Radical Polymerization and Click Chemistry for Surface Modification, *Macromolecules.* **2007**, *40,* 6217-6223.

122. D. E. Achatz, F. J. Heiligtag, X. Li, M. Link and O. S. Wolfbeis, Colloidal Sailica Nanoparticles for Use in Click Chemistry-based Conjugations and Fluorescent Affinity Assays, *Sens. Act. B: Chem.* **2010**, *150,* 211-219.

123. B. I. Dach, H. R. Rengifo, N. J. Turro and J. T. Koberstein, Cross-Linked "Matrix-Free" Nanocomposites from Reactive Polymer-Silica Hybrid Nanoparticles, *Macromolecules.* **2010**, *43,* 6549-6552.

124. P. Tao, Y. Li, A. Rungta, A. Viswanath, J. Gao, B. C. Benicewicz, R. W. Siegel and L. S. Schadler, TiO_2 Nanocomposites with High Refractive Index and Transparency, *J. Mater. Chem.* **2011**, *21,* 18623-18629.

125. Y. Li and Brian C. Benicewicz, Functionalization of Silica Nanoparticles via the Combination of Surface-Initiated RAFT Polymerization and Click Reactions, *Macromolecules.* **2008**, *41,* 7986-7992.

126. Huisgen R., *Angew.Chem.* **1963**, *75,* 604.

127. C. Li, J. Han, C. Y. Ryu and B. C. Benicewicz, A Versatile Method to Prepare RAFT Agent Anchored Substrates and the Preparation of PMMA Grafted Nanoparticles, *Macromolecules.* **2006**, *39,* 3175-3183.

128. M. Kobayashi, R. Matsuno, H. Otsuka, and A. Takahara, Precise Surface Structure Control of Inorganic Solid and Metal Oxide Nanoparticles Through Surface-initiated Radical Polymerization, *Sci. Tech. Adv. Mat.* **2006**, *7,* 617.

129. C. Calebrese, L. Hui, L. S. Schadler and J. K. Nelson, A Review on the Importance of Nanocomposite Processing to Enhance Electrical Insulation, *IEEE Trans. Dielectr. Electr. Insul.* **2011**, *18,* 938-945.

130. D. Kim, J. S. Lee, C. M. F. Barry and L. Mead, Microscopic Measurement of the Degree of Mixing for Nanoparticles in Polymer Nanocomposites by TEM Images, *Microsc. Res. Tech.* **2007**, *70,* 539-546.

131. J.W. Leggoe, Nth-nearest Neighbor Statistics for Analysis of Particle Distribution Data Derived from Micrographs, *Scr. Mater*. **2005**, *53*, 1263-1268

132. N. A. C. Cressie, *Statistics for Spatial Data,* John Wiley and Sons, New York, **1991**.

133. H. S. Khare and D. L. Burris, A Quantitative Method for Measuring Nanocomposite Dispersion, *Polymer.* **2010**, *51,* 719-729.

134. Dispersion Characterization, http://research.me.udel.edu/~dlburris/software/dispersion.html, University of Delaware, (18.09.2013).

135. E. Maire, J. Y. Buffière, L. Salvo, J. J. Blandin, W. Ludwig and J. M. Létang, On the Application of X-ray Microtomography in the Field of Materials Science, *Adv. Eng. Mater.* **2001**, *3*, 539-546.

136. C. L. Lin and J. D. Miller, Cone Beam X-ray Microtomography for Three-dimensional Liberation Analysis in the 21st Century, *Int. J. Miner. Process.* **1996**, *47,* 61-73.

137. J. K. Nelson, *Engineering Dielectrics,* ASTM, Philadelphia, 1983, *2*, 445-520.

138. C. Chauvet and C. Laurent, Weibull Statistics in Short-Term Dielectric-Breakdown of Thin Polyethylene Films, *IEEE Trans. Dielectr. Electr. Insul.* **1993**, *28,* 18-29.

139. L. Dissado, Theoretical Basis for The Statistics of Dielectric-Breakdown, *J. Phys. D*, **1990**, *23,* 1582-1591.

140. R. B. Abernethy, J. E. Breneman, C. H. Medlin and J. L. Reinman, *Weibull Analysis Handbook,* Aero Propulsion Laboratory, Air Force Wright Aeronautical Laboratories, Air Force Systems Command, West Palm Beach, Florida, USA, **1983**.

141. IEC Standard 60250, Recommended methods for the determination of the permittivity and Dielectric Dissipation Factor of Electrical Insulating Materials at Power, Audio and Radio Frequencies Including Metre Wavelengths, *IEC Standard 250.* **1969**.

142. S. J. Laihonen, U. Gafvert, T. Schutte and U. W. Gedde, DC Breakdown Strength of Polypropylene Films: Area Dependence and Statistical Behavior, *IEEE Trans. Dielectr. Electr. Insul.* **2007**, *14,* 275-286.

DEPARTMENT OF CHEMISTRY, UNIVERSITY OF JYVÄSKYLÄ
RESEARCH REPORT SERIES

1. Vuolle, Mikko: Electron paramagnetic resonance and molecular orbital study of radical ions generated from (2.2)metacyclophane, pyrene and its hydrogenated compounds by alkali metal reduction and by thallium(III)trifluoroacetate oxidation. (99 pp.) 1976
2. Pasanen, Kaija: Electron paramagnetic resonance study of cation radical generated from various chlorinated biphenyls. (66 pp.) 1977
3. Carbon-13 Workshop, September 6-8, 1977. (91 pp.) 1977
4. Laihia, Katri: On the structure determination of norbornane polyols by NMR spectroscopy. (111 pp.) 1979
5. Nyrönen, Timo: On the EPR, ENDOR and visible absorption spectra of some nitrogen containing heterocyclic compounds in liquid ammonia. (76 pp.) 1978
6. Talvitie, Antti: Structure determination of some sesquiterpenoids by shift reagent NMR. (54 pp.) 1979
7. Häkli, Harri: Structure analysis and molecular dynamics of cyclic compounds by shift reagent NMR. (48 pp.) 1979
8. Pitkänen, Ilkka: Thermodynamics of complexation of 1,2,4-triazole with divalent manganese, cobalt, nickel, copper, zinc, cadmium and lead ions in aqueous sodium perchlorate solutions. (89 pp.) 1980
9. Asunta, Tuula: Preparation and characterization of new organometallic compounds synthesized by using metal vapours. (91 pp.) 1980
10. Sattar, Mohammad Abdus: Analyses of MCPA and its metabolites in soil. (57 pp.) 1980
11. Bibliography 1980. (31 pp.) 1981
12. Knuuttila, Pekka: X-Ray structural studies on some divalent 3d metal compounds of picolinic and isonicotinic acid N-oxides. (77 pp.) 1981
13. Bibliography 1981. (33 pp.) 1982
14. 6th National NMR Symposium, September 9-10, 1982, Abstracts. (49 pp.) 1982
15. Bibliography 1982. (38 pp.) 1983
16. Knuuttila, Hilkka: X-Ray structural studies on some Cu(II), Co(II) and Ni(II) complexes with nicotinic and isonicotinic acid N-oxides. (54 pp.) 1983
17. Symposium on inorganic and analytical chemistry May 18, 1984, Program and Abstracts. (100 pp.) 1984
18. Knuutinen, Juha: On the synthesis, structure verification and gas chromatographic determination of chlorinated catechols and guaiacols occuring in spent bleach liquors of kraft pulp mill. (30 pp.) 1984
19. Bibliography 1983. (47 pp.) 1984
20. Pitkänen, Maija: Addition of BrCl, B_2 and Cl_2 to methyl esters of propenoic and 2-butenoic acid derivatives and ^{13}C NMR studies on methyl esters of saturated aliphatic mono- and dichlorocarboxylic acids. (56 pp.) 1985
21. Bibliography 1984. (39 pp.) 1985
22. Salo, Esa: EPR, ENDOR and TRIPLE spectroscopy of some nitrogen heteroaromatics in liquid ammonia. (111 pp.) 1985
23. Humppi, Tarmo: Synthesis, identification and analysis of dimeric impurities of chlorophenols. (39 pp.) 1985
24. Aho, Martti: The ion exchange and adsorption properties of sphagnum peat under acid conditions. (90 pp.) 1985
25. Bibliography 1985 (61 pp.) 1986
26. Bibliography 1986. (23 pp.) 1987
27. Bibliography 1987. (26 pp.) 1988
28. Paasivirta, Jaakko (Ed.): Structures of organic environmental chemicals. (67 pp.) 1988
29. Paasivirta, Jaakko (Ed.): Chemistry and ecology of organo-element compounds. (93 pp.) 1989
30. Sinkkonen, Seija: Determination of crude oil alkylated dibenzothiophenes in environment. (35 pp.) 1989
31. Kolehmainen, Erkki (Ed.): XII National NMR Symposium Program and Abstracts. (75 pp.) 1989
32. Kuokkanen, Tauno: Chlorocymenes and Chlorocymenenes: Persistent chlorocompounds in spent bleach liquors of kraft pulp mills. (40 pp.) 1989
33. Mäkelä, Reijo: ESR, ENDOR and TRIPLE resonance study on substituted 9,10-anthraquinone radicals in solution. (35 pp.) 1990
34. Veijanen, Anja: An integrated sensory and analytical method for identification of off-flavour compounds. (70 pp.) 1990
35. Kasa, Seppo: EPR, ENDOR and TRIPLE resonance and molecular orbital studies on a substitution reaction of anthracene induced by thallium(III) in two fluorinated carboxylic acids. (114 pp.) 1990
36. Herve, Sirpa: Mussel incubation method for monitoring organochlorine compounds in freshwater recipients of pulp and paper industry. (145 pp.) 1991
37. Pohjola, Pekka: The electron paramagnetic resonance method for characterization of Finnish peat types and iron (III) complexes in the process of peat decomposition. (77 pp.) 1991

38. Paasivirta, Jaakko (Ed.): Organochlorines from pulp mills and other sources. Research methodology studies 1988-91. (120 pp.) 1992
39. Veijanen, Anja (Ed.): VI National Symposium on Mass Spectrometry, May 13-15, 1992, Abstracts. (55 pp.) 1992
40. Rissanen, Kari (Ed.): The 7. National Symposium on Inorganic and Analytical Chemistry, May 22, 1992, Abstracts and Program. (153 pp.) 1992
41. Paasivirta, Jaakko (Ed.): CEOEC'92, Second Finnish-Russian Seminar: Chemistry and Ecology of Organo-Element Compounds. (93 pp.) 1992
42. Koistinen, Jaana: Persistent polychloroaromatic compounds in the environment: structure-specific analyses. (50 pp.) 1993
43. Virkki, Liisa: Structural characterization of chlorolignins by spectroscopic and liquid chromatographic methods and a comparison with humic substances. (62 pp.) 1993
44. Helenius, Vesa: Electronic and vibrational excitations in some biologically relevant molecules. (30 pp.) 1993
45. Leppä-aho, Jaakko: Thermal behaviour, infrared spectra and x-ray structures of some new rare earth chromates(VI). (64 pp.) 1994
46. Kotila, Sirpa: Synthesis, structure and thermal behavior of solid copper(II) complexes of 2-amino-2- hydroxymethyl-1,3-propanediol. (111 pp.) 1994
47. Mikkonen, Anneli: Retention of molybdenum(VI), vanadium(V) and tungsten(VI) by kaolin and three Finnish mineral soils. (90 pp.) 1995
48. Suontamo, Reijo: Molecular orbital studies of small molecules containing sulfur and selenium. (42 pp.) 1995
49. Hämäläinen, Jouni: Effect of fuel composition on the conversion of fuel-N to nitrogen oxides in the combustion of small single particles. (50 pp.) 1995
50. Nevalainen, Tapio: Polychlorinated diphenyl ethers: synthesis, NMR spectroscopy, structural properties, and estimated toxicity. (76 pp.) 1995
51. Aittola, Jussi-Pekka: Organochloro compounds in the stack emission. (35 pp.) 1995
52. Harju, Timo: Ultrafast polar molecular photophysics of (dibenzylmethine)borondifluoride and 4-aminophthalimide in solution. (61 pp.) 1995
53. Maatela, Paula: Determination of organically bound chlorine in industrial and environmental samples. (83 pp.) 1995
54. Paasivirta, Jaakko (Ed.): CEOEC'95, Third Finnish-Russian Seminar: Chemistry and Ecology of Organo-Element Compounds. (109 pp.) 1995
55. Huuskonen, Juhani: Synthesis and structural studies of some supramolecular compounds. (54 pp.) 1995
56. Palm, Helena: Fate of chlorophenols and their derivatives in sawmill soil and pulp mill recipient environments. (52 pp.) 1995
57. Rantio, Tiina: Chlorohydrocarbons in pulp mill effluents and their fate in the environment. (89 pp.) 1997
58. Ratilainen, Jari: Covalent and non-covalent interactions in molecular recognition. (37 pp.) 1997
59. Kolehmainen, Erkki (Ed.): XIX National NMR Symposium, June 4-6, 1997, Abstracts. (89 pp.) 1997
60. Matilainen, Rose: Development of methods for fertilizer analysis by inductively coupled plasma atomic emission spectrometry. (41 pp.) 1997
61. Koistinen, Jari (Ed.): Spring Meeting on the Division of Synthetic Chemistry, May 15-16, 1997, Program and Abstracts. (36 pp.) 1997
62. Lappalainen, Kari: Monomeric and cyclic bile acid derivatives: syntheses, NMR spectroscopy and molecular recognition properties. (50 pp.) 1997
63. Laitinen, Eira: Molecular dynamics of cyanine dyes and phthalimides in solution: picosecond laser studies. (62 pp.) 1997
64. Eloranta, Jussi: Experimental and theoretical studies on some quinone and quinol radicals. (40 pp.) 1997
65. Oksanen, Jari: Spectroscopic characterization of some monomeric and aggregated chlorophylls. (43 pp.) 1998
66. Häkkänen, Heikki: Development of a method based on laser-induced plasma spectrometry for rapid spatial analysis of material distributions in paper coatings. (60 pp.) 1998
67. Virtapohja, Janne: Fate of chelating agents used in the pulp and paper industries. (58 pp.) 1998
68. Airola, Karri: X-ray structural studies of supramolecular and organic compounds. (39 pp.) 1998
69. Hyötyläinen, Juha: Transport of lignin–type compounds in the receiving waters of pulp mills. (40 pp.) 1999
70. Ristolainen, Matti: Analysis of the organic material dissolved during totally chlorine-free bleaching. (40 pp.) 1999
71. Eklin, Tero: Development of analytical procedures with industrial samples for atomic emission and atomic absorption spectrometry. (43 pp.) 1999

72. Välisaari, Jouni: Hygiene properties of resol-type phenolic resin laminates. (129 pp.) 1999
73. Hu, Jiwei: Persistent polyhalogenated diphenyl ethers: model compounds syntheses, characterization and molecular orbital studies. (59 pp.) 1999
74. Malkavaara, Petteri: Chemometric adaptations in wood processing chemistry. (56 pp.) 2000
75. Kujala Elena, Laihia Katri, Nieminen Kari (Eds.): NBC 2000, Symposium on Nuclear, Biological and Chemical Threats in the 21st Century. (299 pp.) 2000
76. Rantalainen, Anna-Lea: Semipermeable membrane devices in monitoring persistent organic pollutants in the environment. (58 pp.) 2000
77. Lahtinen, Manu: *In situ* X-ray powder diffraction studies of Pt/C, CuCl/C and Cu_2O/C catalysts at elevated temperatures in various reaction conditions. (92 pp.) 2000
78. Tamminen, Jari: Syntheses, empirical and theoretical characterization, and metal cation complexation of bile acid-based monomers and open/closed dimers. (54 pp.) 2000
79. Vatanen, Virpi: Experimental studies by EPR and theoretical studies by DFT calculations of α-amino-9,10-anthraquinone radical anions and cations in solution. (37 pp.) 2000
80. Kotilainen, Risto: Chemical changes in wood during heating at 150-260 °C. (57 pp.) 2000
81. Nissinen, Maija: X-ray structural studies on weak, non-covalent interactions in supramolecular compounds. (69 pp.) 2001
82. Wegelius, Elina: X-ray structural studies on self-assembled hydrogen-bonded networks and metallosupramolecular complexes. (84 pp.) 2001
83. Paasivirta, Jaakko (Ed.): CEOEC'2001, Fifth Finnish-Russian Seminar: Chemistry and Ecology of Organo-Element Compounds. (163 pp.) 2001
84. Kiljunen, Toni: Theoretical studies on spectroscopy and atomic dynamics in rare gas solids. (56 pp.) 2001
85. Du, Jin: Derivatives of dextran: synthesis and applications in oncology. (48 pp.) 2001
86. Koivisto, Jari: Structural analysis of selected polychlorinated persistent organic pollutants (POPs) and related compounds. (88 pp.) 2001
87. Feng, Zhinan: Alkaline pulping of non-wood feedstocks and characterization of black liquors. (54 pp.) 2001
88. Halonen, Markku: Lahon havupuun käyttö sulfaattiprosessin raaka-aineena sekä havupuun lahontorjunta. (90 pp.) 2002
89. Falábu, Dezsö: Synthesis, conformational analysis and complexation studies of resorcarene derivatives. (212 pp.) 2001
90. Lehtovuori, Pekka: EMR spectroscopic studies on radicals of ubiquinones Q-*n*, vitamin K_3 and vitamine E in liquid solution. (40 pp.) 2002
91. Perkkalainen, Paula: Polymorphism of sugar alcohols and effect of grinding on thermal behavior on binary sugar alcohol mixtures. (53 pp.) 2002
92. Ihalainen, Janne: Spectroscopic studies on light-harvesting complexes of green plants and purple bacteria. (42 pp.) 2002
93. Kunttu, Henrik, Kiljunen, Toni (Eds.): 4th International Conference on Low Temperature Chemistry. (159 pp.) 2002
94. Väisänen, Ari: Development of methods for toxic element analysis in samples with environmental concern by ICP-AES and ETAAS. (54 pp.) 2002
95. Luostarinen, Minna: Synthesis and characterisation of novel resorcarene derivatives. (200 pp.) 2002
96. Louhelainen, Jarmo: Changes in the chemical composition and physical properties of wood and nonwood black liquors during heating. (68 pp.) 2003
97. Lahtinen, Tanja: Concave hydrocarbon cyclophane B-prismands. (65 pp.) 2003
98. Laihia, Katri (Ed.): NBC 2003, Symposium on Nuclear, Biological and Chemical Threats – A Crisis Management Challenge. (245 pp.) 2003
99. Oasmaa, Anja: Fuel oil quality properties of wood-based pyrolysis liquids. (32 pp.) 2003
100. Virtanen, Elina: Syntheses, structural characterisation, and cation/anion recognition properties of nano-sized bile acid-based host molecules and their precursors. (123 pp.) 2003
101. Nättinen, Kalle: Synthesis and X-ray structural studies of organic and metallo-organic supramolecular systems. (79 pp.) 2003
102. Lampiselkä, Jarkko: Demonstraatio lukion kemian opetuksessa. (285 pp.) 2003
103. Kallioinen, Jani: Photoinduced dynamics of $Ru(dcbpy)_2(NCS)_2$ – in solution and on nanocrystalline titanium dioxide thin films. (47 pp.) 2004
104. Valkonen, Arto (Ed.): VII Synthetic Chemistry Meeting and XXVI Finnish NMR Symposium. (103 pp.) 2004
105. Vaskonen, Kari: Spectroscopic studies on atoms and small molecules isolated in low temperature rare gas matrices. (65 pp.) 2004
106. Lehtovuori, Viivi: Ultrafast light induced dissociation of $Ru(dcbpy)(CO)_2I_2$ in solution. (49 pp.) 2004
107. Saarenketo, Pauli: Structural studies of metal complexing schiff bases , Schiff base derived

N-glycosides and cyclophane π-prismands. (95 pp.) 2004

108. Paasivirta, Jaakko (Ed.): CEOEC'2004, Sixth Finnish-Russian Seminar: Chemistry and Ecology of Organo-Element Compounds. (147 pp.) 2004
109. Suontamo, Tuula: Development of a test method for evaluating the cleaning efficiency of hard-surface cleaning agents. (96 pp.) 2004
110. Güneş, Minna: Studies of thiocyanates of silver for nonlinear optics. (48 pp.) 2004
111. Ropponen, Jarmo: Aliphatic polyester dendrimers and dendrons. (81 pp.) 2004
112. Vu, Mân Thi Hong: Alkaline pulping and the subsequent elemental chlorine-free bleaching of bamboo (*Bambusa procera*). (69 pp.) 2004
113. Mansikkamäki, Heidi: Self-assembly of resorcinarenes. (77 pp.) 2006
114. Tuononen, Heikki M.: EPR spectroscopic and quantum chemical studies of some inorganic main group radicals. (79 pp.) 2005
115. Kaski, Saara: Development of methods and applications of laser-induced plasma spectroscopy in vacuum ultraviolet. (44 pp.) 2005
116. Mäkinen, Riika-Mari: Synthesis, crystal structure and thermal decomposition of certain metal thiocyanates and organic thiocyanates. (119 pp.) 2006
117. Ahokas, Jussi: Spectroscopic studies of atoms and small molecules isolated in rare gas solids: photodissociation and thermal reactions. (53 pp.) 2006
118. Busi, Sara: Synthesis, characterization and thermal properties of new quaternary ammonium compounds: new materials for electrolytes, ionic liquids and complexation studies. (102 pp.) 2006
119. Mäntykoski, Keijo: PCBs in processes, products and environment of paper mills using wastepaper as their raw material. (73 pp.) 2006
120. Laamanen, Pirkko-Leena: Simultaneous determination of industrially and environmentally relevant aminopolycarboxylic and hydroxycarboxylic acids by capillary zone electrophoresis. (54 pp.) 2007
121. Salmela, Maria: Description of oxygen-alkali delignification of kraft pulp using analysis of dissolved material. (71 pp.) 2007
122. Lehtovaara, Lauri: Theoretical studies of atomic scale impurities in superfluid ^{4}He. (87 pp.) 2007
123. Rautiainen, J. Mikko: Quantum chemical calculations of structures, bonding, and spectroscopic properties of some sulphur and selenium iodine cations. (71 pp.) 2007
124. Nummelin, Sami: Synthesis, characterization, structural and retrostructural analysis of self-assembling pore forming dendrimers. (286 pp.) 2008
125. Sopo, Harri: Uranyl(VI) ion complexes of some organic aminobisphenolate ligands: syntheses, structures and extraction studies. (57 pp.) 2008
126. Valkonen, Arto: Structural characteristics and properties of substituted cholanoates and *N*-substituted cholanamides. (80 pp.) 2008
127. Lähde, Anna: Production and surface modification of pharmaceutical nano- and microparticles with the aerosol flow reactor. (43 pp.) 2008
128. Beyeh, Ngong Kodiah: Resorcinarenes and their derivatives: synthesis, characterization and complexation in gas phase and in solution. (75 pp.) 2008
129. Välisaari, Jouni, Lundell, Jan (Eds.): Kemian opetuksen päivät 2008: uusia oppimisympäristöjä ja ongelmalähtöistä opetusta. (118 pp.) 2008
130. Myllyperkiö, Pasi: Ultrafast electron transfer from potential organic and metal containing solar cell sensitizers. (69 pp.) 2009
131. Käkölä, Jaana: Fast chromatographic methods for determining aliphatic carboxylic acids in black liquors. (82 pp.) 2009
132. Koivukorpi, Juha: Bile acid-arene conjugates: from photoswitchability to cancer cell detection. (67 pp.) 2009
133. Tuuttila, Tero: Functional dendritic polyester compounds: synthesis and characterization of small bifunctional dendrimers and dyes. (74 pp.) 2009
134. Salorinne, Kirsi: Tetramethoxy resorcinarene based cation and anion receptors: synthesis, characterization and binding properties. (79 pp.) 2009
135. Rautiainen, Riikka: The use of first-thinning Scots pine (*Pinus sylvestris*) as fiber raw material for the kraft pulp and paper industry. (73 pp.) 2010
136. Ilander, Laura: Uranyl salophens: synthesis and use as ditopic receptors. (199 pp.) 2010
137. Kiviniemi, Tiina: Vibrational dynamics of iodine molecule and its complexes in solid krypton - Towards coherent control of bimolecular reactions? (73 pp.) 2010
138. Ikonen, Satu: Synthesis, characterization and structural properties of various covalent and non-covalent bile acid derivatives of N/O-heterocycles and their precursors. (105 pp.) 2010
139. Siitonen, Anni: Spectroscopic studies of semiconducting single-walled carbon nanotubes. (56 pp.) 2010
140. Raatikainen, Kari: Synthesis and structural studies of piperazine cyclophanes –

Supramolecular systems through Halogen and Hydrogen bonding and metal ion coordination. (69 pp.) 2010

141. Leivo, Kimmo: Gelation and gel properties of two- and three-component Pyrene based low molecular weight organogelators. (116 pp.) 2011
142. Martiskainen, Jari: Electronic energy transfer in light-harvesting complexes isolated from *Spinacia oleracea* and from three photosynthetic green bacteria *Chloroflexus aurantiacus*, *Chlorobium tepidum*, and *Prosthecochloris aestuarii*.(55 pp.) 2011
143. Wichmann, Oula: Syntheses, characterization and structural properties of [O,N,O,X´] aminobisphenolate metal complexes. (101 pp.) 2011
144. Ilander, Aki: Development of ultrasound-assisted digestion methods for the determination of toxic element concentrations in ash samples by ICP-OES. (58 pp.) 2011
145. The Combined XII Spring Meeting of the Division of Synthetic Chemistry and XXXIII Finnish NMR Symposium. Book of Abstracts. (90 pp.) 2011
146. Valto, Piia: Development of fast analysis methods for extractives in papermaking process waters. (73 pp.) 2011
147. Andersin, Jenni: Catalytic activity of palladium-based nanostructures in the conversion of simple olefinic hydro- and chlorohydrocarbons from first principles. (78 pp.) 2011
148. Aumanen, Jukka: Photophysical properties of dansylated poly(propylene amine) dendrimers. (55 pp.) 2011
149. Kärnä, Minna: Ether-functionalized quaternary ammonium ionic liquids – synthesis, characterization and physicochemical properties. (76 pp.) 2011
150. Jurček, Ondřej: Steroid conjugates for applications in pharmacology and biology. (57 pp.) 2011
151. Nauha, Elisa: Crystalline forms of selected Agrochemical actives: design and synthesis of cocrystals. (77 pp.) 2012
152. Ahkola, Heidi: Passive sampling in monitoring of nonylphenol ethoxylates and nonylphenol in aquatic environments. (92 pp.) 2012
153. Helttunen, Kaisa: Exploring the self-assembly of resorcinarenes: from molecular level interactions to mesoscopic structures. (78 pp.) 2012
154. Linnanto, Juha: Light excitation transfer in photosynthesis revealed by quantum chemical calculations and exiton theory. (179 pp.) 2012
155. Roiko-Jokela, Veikko: Digital imaging and infrared measurements of soil adhesion and cleanability of semihard and hard surfaces. (122 pp.) 2012
156. Noponen, Virpi: Amides of bile acids and biologically important small molecules: properties and applications. (85 pp.) 2012
157. Hulkko, Eero: Spectroscopic signatures as a probe of structure and dynamics in condensed-phase systems – studies of iodine and gold ranging from isolated molecules to nanoclusters. (69 pp.) 2012
158. Lappi, Hanna: Production of Hydrocarbon-rich biofuels from extractives-derived materials. (95 pp.) 2012
159. Nykänen, Lauri: Computational studies of Carbon chemistry on transition metal surfaces. (76 pp.) 2012
160. Ahonen, Kari: Solid state studies of pharmaceutically important molecules and their derivatives. (65 pp.) 2012
161. Pakkanen, Hannu: Characterization of organic material dissolved during alkaline pulping of wood and non-wood feedstocks (76 pp.) 2012
162. Moilanen, Jani: Theoretical and experimental studies of some main group compounds: from closed shell interactions to singlet diradicals and stable radicals. (80 pp.) 2012
163. Himanen, Jatta: Stereoselective synthesis of Oligosaccharides by *De Novo* Saccharide welding. (133 pp.) 2012
164. Bunzen, Hana: Steroidal derivatives of nitrogen containing compounds as potential gelators.(76 pp.) 2013
165. Seppälä, Petri: Structural diversity of copper(II) amino alcohol complexes. Syntheses, structural and magnetic properties of bidentate amino alcohol copper(II) complexes. (67 pp.) 2013
166. Lindgren, Johan: Computational investigations on rotational and vibrational spectroscopies of some diatomics in solid environment. (77 pp.) 2013
167. Giri, Chandan: Sub-component self-assembly of linear and non-linear diamines and diacylhydrazines, formulpyridine and transition metal cations. (145 pp.) 2013
168. Riisiö, Antti: Synthesis, Characterization and Properties of Cu(II)-, Mo(VI)- and U(VI) Complexes With Diaminotetraphenolate Ligands. (51 pp.) 2013
169. Kiljunen, Toni (Ed.): Chemistry and Physics at Low Temperatures. Book of Abstracts. (103 pp.) 2013
170. Hänninen, Mikko: Experimental and Computational Studies of Transition Metal Complexes with Polydentate Amino- and Aminophenolate Ligands: Synthesis, Structure, Reactivity and Magnetic Properties. (66 pp.) 2013

171. Antila, Liisa: Spectroscopic studies of electron transfer reactions at the photoactive electrode of dye-sensitized solar cells. (53 pp.) 2013

172. Kemppainen, Eeva: Mukaiyama-Michael reactions with α-substituted acroleins – a useful tool for the synthesis of the pectenotoxins and other natural product targets. (190 pp.) 2013